Variability in copepod trophic levels and feeding selectivity based on stable isotope analysis in Gwangyang Bay off the southern coast of Korea

Mianrun Chen[1,2], Dongyoung Kim[2], Hongbin Liu[3], Chang-Keun Kang[2]

[1]South China Sea Institute of Planning and Environmental Research, South China Sea Branch, SOA, Guangzhou, P.R. China
[2]School of Earth Sciences & Environmental Engineering, Gwangju Institute of Science and Technology, Gwangju 61005, Republic of Korea
[3]Division of Life Science, The Hong Kong University of Science and Technology, Clear Water Bay, Kowloon, Hong Kong SAR

Correspondence to: Chang-Keun Kang (ckkang@gist.ac.kr)

Abstract. Trophic preference (i.e., food resources and trophic levels) of different copepod groups was assessed along a salinity gradient in the temperate estuarine Gwangyang Bay of Korea, based on seasonal investigation of taxonomic results in 2015 and stable isotope analysis incorporating multiple linear regression models. The δ^{13}C and δ^{15}N values of copepods in the bay displayed significant spatial heterogeneity as well as seasonal variations, which were indicated by their significant relationships with salinity and temperature, respectively. Both spatial and temporal variations reflected those in isotopic values of food sources. The major calanoid groups (marine calanoids and brackish water calanoids) had a mean trophic level of 2.2 relative to nanoplankton as the basal food source, similar to the bulk copepod assemblage; however, they had dissimilar food sources based on the different δ^{13}C values. Calanoid isotopic values indicated a mixture of different genera including species with high δ^{15}N values (e.g., *Labidocera, Sinocalanus*, and *Tortanus*), moderate values (*Calanus sinicus, Centropages, Paracalanus*, and *Acartia*), and relatively low δ^{15}N values (*Eurytemora pacifica* and *Pseudodiaptomus*). Feeding preferences of different copepods probably explain these seasonal and spatial patterns of the community trophic niche. Bayesian mixing model calculations based on source materials of two size fractions of particulate organic matter (nanoplankton at < 20 μm vs microplankton at 20–200 μm) indicated that *Acartia* and *Centropages* preferred large particles, *Paracalanus, Calanus, Eurytemora*, and *Pseudodiaptomus* apparently preferred small particles. *Tortanus* was typically carnivorous with low selectivity on different copepods. *Labidocera* preferred marine calanoids *Acartia, Centropages,* and harpacticoids, and on the other hand, *Sinocalanus* and *Corycaeus* preferred brackish calanoids *Paracalanus* and *Pseudodiaptomus*. Overall, our results depict a simple energy flow of the planktonic food web of Gwangyang Bay: from primary producers (nanoplankton) and a mixture of primary producers and herbivores (microplankton), through omnivores (*Acartia, Calanus, Centropages,* and *Paracalanus*) and detrivores (*Pseudodiaptomus, Eurytemora,* and *harpacticoids*) to carnivores (*Corycaeus, Tortanus, Labidocera*, and *Sinocalanus*).

1 Introduction

Mesozooplankton constitute essential trophic mediators of marine food webs in transferring energy and materials by linking the microbial food web to higher trophic levels. Copepods are a diverse assemblage dominating mesozooplankton communities. With broad feeding spectra and flexible feeding strategies, the bulk copepod assemblage displays varying degree of herbivory/omnivory/carnivory, depending on dominant species or groups (Graeve et al., 1994; Sell et al., 2001; Turner, 2004; Vadstein et al., 2004; Gifford et al., 2007; Chen et al., 2017). The role of copepods in planktonic food webs can be determined by their overall trophic levels (TLs) relative to primary producers. In turn, the TL of a diverse copepod assemblage is balanced from different groups with different feeding preferences and are ultimately determined by species composition. Because copepods rely significantly on phytoplankton as prey, the seasonal and spatial changes in the composition and availability of phytoplankton determine the abundance and feeding behavior of the copepod assemblages.

The most dominant copepod species, such as *Neocalanus*, *Calanus*, *Temora*, and *Paracalanus*, are filter-feeders that perform a size-selective feeding behavior depending on particles effectively retained by feeding appendages of copepods. Large phytoplankton (> 20 μm; mainly diatoms and dinoflagellates) are generally grazed at high rates by copepods, as shown by many field studies in coastal and estuarine waters (e.g., Liu et al., 2005a, b; Chen et al., 2017). Many other field studies have reported that omnivorous species dominate copepod assemblages because of high feeding selectivity on larger microzooplankton that are considered to have higher nutritional quality (e.g., Berk et al., 1977; Fessenden and Cowles, 1994; Calbet and Saiz, 2005; Gifford et al., 2007; Chen et al., 2013). These omnivorous copepods might induce increases in phytoplankton levels indirectly through trophic cascades as they graze intensely on microzooplankton (e.g., ciliates and heterotrophic dinoflagellates) (Nejstgaard et al., 2001; Stibor et al., 2004; Sommer and Sommer, 2006; Zöllner et al., 2009; Chen et al., 2011, 2013). Therefore, the assessment of the trophic position (herbivores, omnivores, or carnivores) of copepods within a complex planktonic food web is critical to understand the ecological relationships between predators and prey.

Stable isotope analysis (SIA) is a reliable technique providing insight into the trophic positions of copepods relative to basal food sources (Grey et al., 2001; Sommer et al., 2005; Hannides et al., 2009; Kürten et al., 2011). Isotopic comparisons with food sources enable us to analyze prey selectivity during predators' feeding history as well as within food web structures (Fry, 2006; Layman et al., 2012). In general, the carbon stable isotope ratio (δ^{13}C) can be useful for tracing food sources because of small fractionation (0.5–1‰ per TL) during trophic transfer, particularly when different food sources at a given period in a specific system have distinct δ^{13}C values. By contrast, the nitrogen stable isotope ratio (δ^{15}N) can be useful for estimating relative TLs because δ^{15}N values of consumers generally increase with TL (an average 3.2‰ of enrichment per TL; Post, 2002; Michener and Kaufman, 2007). The development of linear mixing models and the Bayesian mixing model has allowed researchers to predict the proportions of different food sources in the diets assimilated by grazers (Phillips and Koch, 2002; Phillips and Gregg, 2003; Moore and Semmens, 2008; Ward et al., 2010; Parnell et al., 2010, 2013).

Coastal and estuarine environments often experience rapid fluctuations of inorganic carbon and nitrogen inputs in response to diverse oceanographic processes (e.g., coastal currents, upwelling, tidal mixing, and river discharges), which drive spatial and

seasonal heterogeneities in biogeochemical dynamics and isotopic signatures (Rolff, 2000). Indeed, the δ^{13}C values of suspended particulate organic matter (POM) in estuarine systems increase progressively from the head to the mouth of each estuary because of the lower δ^{13}C values in terrestrial carbon or sewage materials through river discharge (Cifuentes et al., 1988). In contrast, the δ^{15}N values of primary producers increase from being nutrient-sufficient (high fractionation) to nutrient-

5 limiting (low fractionation) and are especially high in anthropogenic wastewater nitrogen inputs (McClelland et al., 1997). In addition, different phytoplankton groups utilize different nitrogen sources with different enrichment factors, possibly offering different isotopic pools to grazers (Gearing et al., 1984; Rolff, 2000; Montoya et al., 2002). For example, diatoms primarily utilize nitrate with varying fractionation factor on ^{15}N (0.7–6.2‰) depending on species (Waser, et al, 1998; Needoba et al., 2003), while flagellates primarily utilize ammonia with enrichment factor of 6.5–8‰ (Montoya et al., 1991).

10 Given that isotopic values of copepods vary in association with copepods' food source by one or two increases in TL values, seasonal and spatial patterns generally follow the trends of their food sources or dominant prey (Grey et al., 2001; Montoya et al., 2002; Kürten et al., 2011). Higher δ^{15}N values of copepods caused by fractionation rather than food source or by averaging from mixed food sources are evident considering the lowered isotopic values of fecal pellets (Checkley and Entzeroth, 1985; Checkley and Miller, 1989; Tamelander et al., 2006). Furthermore, the effect of the microbial food web on the elevated δ^{15}N

15 values of copepods cannot be ignored (Rolff, 2000; Kürten et al., 2011). Therefore, variations in isotope signatures of both copepods and POM (including phytoplankton, bacteria, ciliates, and detritus) help to depict the biogeochemical cycles of specific systems (Grey et al., 2001; Montoya et al., 2002; Francis et al., 2011). Nevertheless, because copepods graze preferentially on larger phytoplankton (diatoms and dinoflagellates) and microzooplankton (ciliates and heterotrophic dinoflagellates), we hypothesize that isotopic values of the copepod assemblage will be much closer to those of larger rather

20 than smaller food source plankton.

However, high diversity of the assemblage and size overlap among different species make it hard to determine the relative trophic positions of different subgroups or species. Isotope analysis for different subgroups requires great expertise in isolating species from highly complex mixtures. Moreover, the number of individuals of a specific genus is often insufficient for analysis because of limited instrument sensitivity. Thus, to our knowledge, direct comparisons of different mesozooplankton groups or

25 copepod species are seldom found in the literature (Schmidt et al., 2003; Sommer et al., 2005; Hannides et al., 2009). Here, we estimated isotope values of different copepods by mass balancing linear mixing models from values of bulk samples and taxonomic data of copepods. The allocated masses of calanoids and cyclopoids were achieved from literature and empirical formulas.

Overall, we aimed (1) to understand the seasonal variations and spatial heterogeneity of copepod δ^{13}C and δ^{15}N values in a

30 temperate estuarine system (Gwangyang Bay, Korea); (2) to compare the trophic positions of different copepods; and finally (3) to elucidate the compositions of two major size classes (<20 μm and >20 μm) of POM in grazer diets. The dietary composition (nano-vs microplankton) of copepods was estimated using Bayesian isotopic mixing models (Parnell et al., 2010,

2013). The results of this study will provide insights into trophic preference information (i.e., food resources and trophic levels) for different copepod groups and help in understanding the biogeochemistry of this estuarine system.

2 Materials and methods

2.1 Study area

5   Gwangyang Bay is a semi-enclosed bay system, located on the southern coast of the Korean Peninsula, and is one of the most industrialized coastal areas exposed to anthropogenic pressure. It starts from Seomjin River through Yeosu Channel (between Yeosu Peninsula and Namhae Island) to open ocean (the East China Sea). The bay area covers approximately 145 km^2 and water depth is generally shallow at 2.4–8.0 m in the northern upper-middle Seomjin River estuarine channel compared with 10–30 m in the deep bay channel (Kim et al., 2014). The annual freshwater discharges of Seomjin River are 10.7–39.3 × 10^8

10   tons. The seasonality of nutrient input from the catchment area (ca. 5 × 10^3 km^2), including agricultural and forested land, is profound (Kwon et al., 2002). The wet season starts from late spring and the discharge peaks during the summer monsoon period.

Accordingly, the maximum median river discharge varies from 30–95 m^3 s^{-1} in the dry season to 300–400 m^3 s^{-1} in the summer monsoon, with an annual mean of c.120 m^3 s^{-1} (Kim et al., 2014). The tidal cycle of the bay is semidiurnal with maximum

15   ranges of 3.40 m during spring tides and 1.10 m during neap tides. Tidal currents from the Yeosu Channel also strongly influence the system and approximately 82% of the Seomjin River flux is discharged toward this channel. Overall, increasing industrial pollution facilitates eutrophic conditions in the estuarine and related bay waters. Diatoms dominate in the phytoplankton community and density is high in the middle part of the Gwangyang Bay (Kim et al., 2009; data from our parallel study not shown). The distribution patterns of copepods in the Seomjin River during summer were represented by

20   three main salinity zones: an oligohaline zone (predominated by *Pseudodiaptomas koreanus*, *Sinocalanus tenellus*, and *Tortanus dextrilobatus*), a mesohaline zone (predominated by *Acartia ohtsukai* and *Acartia forticrusa*), and a polyhaline zone (predominated by *Acartia erythraea, Calanus sinicus, Centropages dorsispinatus, Labidocera rotunda*, and *Paracalanus parvus*) (Park et al., 2015).

2.2 Sampling and processing

25   Surface water and net-tow samples were collected seasonally (February, May, August, and November) at nine stations from the head to the mouth of Gwangyang Bay in 2015 (Fig. 1). The stations were chosen based on salinity regime and different geographic characteristics. Stations 1–3 were located in the Seomjin River, stations 4 and 5 were in Gwangyang Bay (the middle part of the estuary), and stations 6–9 were located from the offshore deep-bay channel to the southern mouth of the estuary. On each sampling occasion, water temperature and salinity were determined in situ using an YSI Model 85 probe

30   (YSI Inc., Yellow Springs, OH, USA).

4

Zooplankton taxonomic samples were collected during daytime by net towing using a plankton net (45 cm diameter, 200 μm mesh size) equipped with a flowmeter (Model 2030R Mechanical Flowmeter, General Oceanics Inc., Miami, FL) and gently hauled horizontally at a subsurface depth of 0.5–1 m with the ship speed at about 1 knot (0.5 m s^{-1}). The average volume filtered per tow was 16.7 ± 5.1 m^3 (mean ± se). Samples were fixed in formalin solution with a final concentration of 5% and then identified and enumerated under a stereomicroscope (SMZ 645; Nikon, Tokyo, Japan) in the laboratory. At each station, one additional net tow was collected for isotope analysis. After collection, specimens were transferred immediately into plastic bottles and preserved in a refrigerator (4 °C) until analysis. In the laboratory, subsamples were picked out from the mixed zooplankton samples under a dissecting microscope. Easily distinguishable zooplankton groups such as harpacticoids were separated from a mixture of calanoids and cyclopoids. Copepodites were counted but grouped together with adults. All subsamples were lyophilized and then homogenized by pulverizing them with a mortar and pestle before isotope analysis.

POM in surface water (0.5–1 m depth) was collected using a 5-l Niskin bottle at a midday high tide at the same time as zooplankton collection. Approximately 20 l seawater collected was first screened through a 200 μm Nitex mesh to remove zooplankton and large-sized particles. The pre-screened water samples were transported to the laboratory as soon as possible within 1–2 h. In the laboratory, water samples were filtered again through a 20 μm Nitex mesh and then filtered onto pre-combusted (450 °C for 4 h) Whatman GF/F glass fiber filters to determine isotope ratios of fine POM (< 20 μm) representing pico- and nano-sized plankton. To obtain enough plankton cells for isotope analysis of coarse POM ($\geq$ 20μm), we collected POM samples by net towing with a plankton net of 50 cm diameter and 20 μm mesh size. After collection, each sample was pre-filtered through a 200 μm Nitex mesh to remove large particles and zooplankton. Both size fractions of samples were prepared in duplicate. Samples for δ^{13}C measurements were acidified by fuming for about 5 h over concentrated HCl in a vacuum desiccator to remove carbonates, while the samples for δ^{15}N measurements were not acidified. All the samples were lyophilized and pulverized with a mortar and pestle before isotope analysis.

For chlorophyll a (Chl a) determination, 1-l subsamples of surface water were filtered through Waterman GF/F glass fiber filters. The filters for Chl a (including other photosynthetic pigments) were extracted with 95% methanol (5 ml) for 12 h in the dark at −20 °C and sonicated for 5 min to foster cell disruption. Aliquots of 1 ml of the supernatants were mixed with 300 μl of water; 100 μl of this solution was analyzed by reverse-phase high performance liquid chromatography (HPLC, LC-20A HPLC system, Shimadzu Co., Kyoto, Japan) using a Water Symmetry C$_8$ (4.6 × 150 mm, particle size: 3.5 μm, 100 Å pore size) column (Waters, Milford, MA, USA) and a method derived from Zapata et al. (2000). Quantification of standard pigments was calculated by spectrophotometer with the known specific extinction coefficients after Jeffrey at al. (1997). Sample peaks were identified based on their retention time compared with those of pure standards. Further details on analysis, calibration, and quantification have been given elsewhere (Lee et al., 2011; Kwak et al., 2017).

2.3 Isotope analysis

For measurements of carbon and nitrogen stable isotope ratios, all pre-treated samples were analyzed using a continuous-flow

isotope ratio mass spectrometer (CF-IRMS; Isoprime100, Cheadle, UK) connected to an elemental analyzer (vario Micro cube, Hanau, Germany) following the procedure described by Park et al. (2016). Briefly, powdered samples were sealed in tin combustion cups and filter samples were wrapped with a tin plate. All prepared samples were put into the elemental analyzer to oxidize at high temperature (1030 °C). CO_2 and N_2gaseswere introduced into the CF-IRMS with the carrier being helium gas. Data of isotope values are shown in terms of δX, indicating the relative differences between isotope ratios of the sample and conventional standard reference materials (Vienna Pee Dee Belemnite for carbon, and atmospheric N_2 for nitrogen), which were calculated by the following equations:$\delta X = [(R_{sample}/R_{standard}) - 1] \times 10^3$, where X is ^{13}C or ^{15}N and $R_{sample}$and $R_{standard}$ are the ratios of heavy to light isotope for samples and standards, respectively. International standards of sucrose (ANU $C_{12}H_{22}O_{11}$; National Institute of Standards and Technology (NIST), Gaithersburg, MD, USA) for carbon, and ammonium sulfate ($[NH_4]_2SO_4$; NIST) for nitrogen, were used for calibration after analyzing every 5–10 samples. The analytical precision for 20 replicates of urea were approximately ≤ 0.1‰ and ≤ 0.05‰ for δ^{13}C and δ^{15}N, respectively.

2.4 Data analysis

We used multiple linear regression to assign the isotopic value to each species from a mixture sample. As we did not measure the dry weights each species directly, we calculated them using published empirical equation of the relationship between body length and dry weight of each species and we searched literature for the range of body length and their living environment of each species in the ′World of Copepods Database′ and related references (Table S1). Those calanoid species primarily living marine environment based on the definition of ′World of Copepods Database′ and related references were grouped as marine calanoids in this paper including *Acartia hudsonica*, *Acartia o*morii, *Bestiolina coreana*, *Calanus sinicus, Clausocalanus furcatus, Centropages abdominalis, Centropages dorsispinatus, Paracalanus aculeatus, Paraeuchaeta plana, Labidocera rotunda*, *Labidocera euchaeta*, *Tortanus dextrilobatus*, and *Tortanus forcipatus*. The group of brackish calanoids included *Acartia ohtsukai*, *Acartia erythraea*, *Eurytemora Pacifica*, *Paracalanus parvus*, *Pseudodiaptomus koreanus*, *Pseudodiaptomus marinus* and *Sinocalanus tenellus*.

Assuming that the proportion we picked to do isotope analysis was the same as the proportion in samples for composition analysis, once the weights of different groups or different genera/species were assigned, we computed the isotope ratio for each group by multiple linear regression models as in the following equations:

$$m \times \delta^{13}C = m_1 \times \delta^{13}C_1 + m_2 \times \delta^{13}C_2 + m_3 \times \delta^{13}C_3 + m_X \times \delta^{13}C_X + error, \tag{1}$$

$$m \times \delta^{15}N = m_1 \times \delta^{15}N_1 + m_2 \times \delta^{15}N_2 + m_3 \times \delta^{15}N_3 + m_X \times \delta^{15}N_X + error, \tag{2}$$

where m is the weight of the total community and $m_1 - m_X$ are the weight of different groups or genera of each group. $\delta^{13}C_1 - \delta^{13}C_X$and $\delta^{15}N_1 - \delta^{15}N_X$ are the δ^{13}C and δ^{15}N values of each group or genus, respectively. We used R software to do the estimation using the whole sampling data set. Insignificant results for sparse species, such as *Bestiolina coreana,*

Clausocalanus furcatus, *Paraeuchaeta plana, Oithona davisae,* and *Oncaea venella*, found in Gwangyang Bay are not tested separately, while they were incorporated to respective groups based on their living environment.

Given that the isotopic values of consumers come from their diets and thereby from mixed proportions of different sources, the proportions of each source could be simulated by linear mixing models with a fractionation factor (also called a trophic enrichment factor). For instance, a mass balance mixing model is given by:

$$\delta^{13}C_{consumer} = f_1\delta^{13}C_{source1} + f_2\delta^{13}C_{source2} + \cdots + f_n\delta^{13}C_{source\,n} + \alpha_{Carbon}, \tag{3}$$

$$\delta^{15}N_{consumer} = f_1\delta^{15}N_{source1} + f_2\delta^{15}N_{source2} + \cdots + f_n\delta^{15}N_{source\,n} + \alpha_{Nitrogen}, \tag{4}$$

$$f_1 + f_2 + \cdots + f_n = 1, \tag{5}$$

where f_1-f_n are the proportion of different sources, and α_{Carbon} and $\alpha_{Nitrogen}$ are trophic enrichment factors for δ^{13}C and δ^{15}N values, respectively.

Here, a Bayesian isotopic mixing model (available as an open source Stable Isotope Analysis package in R: SIAR) was performed to estimate the relative contribution of nanoplankton (defined by fine POM in the present study) and microplankton (coarse POM) to the copepod diets, as well as copepods to the carnivore diets (Parnell et al., 2010, 2013). The model assumes that each isotopic ratio of consumers follows the pattern of a Gaussian distribution with an unknown mean and standard deviation. The structure of mean values of consumers is a weighted combination of the food sources' isotopic values. The weights make up dietary proportions (given by a Dirichlet prior distribution). The standard deviation is divided up between the uncertainty around the fractionation corrections and the natural variability between all individuals within a defined group (Parnell et al., 2010, 2013). Because the values of consumers calculated from bulk copepod samples using the previous multiple linear regression models were only means and standard errors, we generated a vector consisting of 250 numbers for each group by a random normal distribution function. We then used the default iteration numbers (iterations = 500,000, burin = 50,000) provided by the SIAR package to perform our analysis. Fractionation factors used in the model estimation were estimated by difference of TLs multiplying with 3‰ per TL for δ^{15}N and with 0.5‰ per TL for δ^{13}C, respectively. TLs were calculated from the δ^{15}N difference between consumer and source as follows (Post, 2002): $(TL = 1 + (\delta^{15}N_{consumer} - \delta^{15}N_{source})/3)$. Concentrations of isotope per mass among different diets (nanoplankton, microplankton, and major copepod genera) were not considered in this study. Model fitting was done via a Markov Chain Monte Carlo (MCMC) protocol that produces simulations of plausible values of the dietary proportions of each source. More details on model simulation can be found elsewhere (Parnell et al., 2010, 2013).

All statistical analyses were performed using R 3.4.0 software (https://cran.r-project.org/bin/windows/base/). Regression analyses of copepod isotopic values were performed by generalized additive models (GAMs) using the *mgcv* library (Wood and Wood, 2015). Data were smoothed by cubic regression splines and fitted by the family of Gaussian. One-way analysis of variance (ANOVA) was adopted to test seasonal differences in environmental factors and copepod abundances, and Student's *t*-tests were used to test for significant differences in mean δ^{13}C and δ^{15}N values between nano- and microplankton. Before

applying ANOVA and *t*-tests, the data were tested for normality of distribution and equal variance; significance was assumed at $P = 0.05$. For the coefficients of variation, we calculated them by dividing the standard error with mean value.

3 Results

3.1 Environmental variability and zooplankton abundances

Environmental factors including temperature, salinity, Chl *a* levels, copepod abundance, dominant species, and percentages of total copepods are shown in Table 1. Water temperature was significantly higher in summer and lower in winter (ANOVA, $P < 0.001$). Spatial variability of salinity was significant, with extremely low values at stations 1 and 2 (the river mouth) and then the values gradually increased to station 5 (the middle of the bay). Chl *a* concentrations ranged from 0.1 to 6.8μg l^{-1} and they were significantly higher in spring and summer than in winter and autumn (ANOVA, $P < 0.01$). The highest Chl *a* concentration occurred in the middle of the bay during the spring, while the lowest concentration was found at the river station during the autumn. Seasonal variability of copepod abundance was significant (ANOVA, $P < 0.01$), with higher abundances in winter when temperatures and Chl *a* concentrations were low.

Detailed abundance composition of copepods is shown in Table S2. Seasonal and spatial variations of dominant species (>10% of total abundance) of copepods were apparent (Table 1). The marine calanoid *Acartia* dominated at the river mouth to the middle part of the bay, while *Paracalanus* dominated at the mouth of the bay during winter. *Acartia* also dominated at the most highly saline stations in summer, except for station 7, where the community was dominated by *Labidocera rotunda*. A brackish water-preferring calanoid species, *Pseudodiaptomus,* dominated stations 1 and 2 at the river mouth in spring and another brackish calanoid species, *Sinocalanus*, dominated station 1 in autumn. At the river-mouth stations in summer, copepods were unexpectedly dominated by the marine calanoid species *Tortanus dextrilobatus*. The cyclopoid species *Corycaeus affinis* mainly dominated the most highly saline stations in spring and autumn.

3.2 Variability of plankton δ¹³C and δ¹⁵N values

The δ¹³C values of size-fractionated plankton (< 20 and 20–200 μm) and mixed copepod samples showed distinct spatial variations in each season (Fig. 2A–C). The δ¹³C values of nanoplankton (< 20 μm POM) ranged from −27.6 to −19.4‰ with a mean of −22.7‰ (Fig. 2A). The lowest δ¹³C value of nanoplankton was found at station 1 (the upper stream station of Seomjin River) in spring and the highest at station 9 (the mouth of the estuary) in summer. The δ¹³C values of microplankton (20–200 μm POM) ranged from −26.3 to −17.8‰ with a mean of −20.8‰ (Fig. 2B), being significantly higher than those of nanoplankton (paired *t*-test, $t = 7.6$, $P < 0.001$). Its lowest δ¹³C value was found at station 2 in spring and the highest at station 8 in winter. Overall, similar to nanoplankton, the microplankton δ¹³C values were more negative at the river portion (stations 1–3) and less negative at the mouth of the estuary (stations 7–9). The δ¹³C values of mixed copepods ranged from −25.9 to −16.4‰, with a mean of −20.1‰ (Fig. 2C). The lowest at station 1 in autumn and the highest at station 8 in summer. The

spatial variability of copepod δ^{13}C values followed the pattern of POM δ^{13}C values. However, the copepod δ^{13}C values were significantly higher than those of nanoplankton (paired t-test, $t = 8.6$, $P < 0.001$) and microplankton ($t = 3.1$, $P = 0.004$). Their δ^{13}C values were higher in summer and winter than in spring and autumn. At stations 1–3, river input lowered the δ^{13}C values of nanoplankton during the wet season (spring to summer). At stations 4–9, significantly lower δ^{13}C values were observed in

5　autumn than in other seasons (ANOVA, $F = 13.4$, $P < 0.001$). For copepods, the autumn values were significantly lower than those in other seasons (ANOVA, $F = 5.9$, $P = 0.004$).

The δ^{15}N values exhibited wider fluctuations than δ^{13}C values (coefficients of variation = 29.3% vs. 9.0%, 21.5% vs. 11.8%, and 18.8% vs. 13.1% for nanoplankton, microplankton, and copepods, respectively). The δ^{15}N values of nanoplankton ranged from 3.2‰ (station 4 in summer) to 8.8‰ (station 1 in winter) with a mean of 5.6‰ (Fig. 2D). There were distinct patterns in

10　the three locations of the bay. The δ^{15}N values tended to decline with distance from the river mouth, then increased in the middle of the bay, and decreased again toward the mouth of the estuary. The nanoplankton δ^{15}N values were higher in winter than in other seasons (paired t-test, $t = 5.4$, $P = 0.001$ for spring; $t = 3.0$, $P = 0.017$ for summer; $t = 4.1$, $P = 0.004$ for autumn). As indicated by regression analyses between the distribution of nanoplankton δ^{15}N and environmental factors (Table 2), significant increases in the nanoplankton δ^{15}N values depend on ammonia (GAM, $F = 4.1$, $P = 0.029$) and Chl a (GAM, $F =$

15　3.8, $P = 0.044$). In addition, the seasonal distribution of nanoplankton δ^{15}N values was well indicated by their relationship with temperature among different seasons (GAM, $F = -5.5$, $P = 0.013$), decreasing the values in summer to autumn.

Mean δ^{15}N value of microplankton (7.6‰), ranging from 4.8‰ (station 2 in spring) to 10.2‰ (station 6 in spring), was significantly higher than that of nanoplankton (paired t-test, $t = 4.9$, $P < 0.001$). The microplankton δ^{15}N values were higher in summer than in other seasons (ANOVA, $F = 4.6$, $P = 0.009$), with the spatial trend vanishing in summer. Indeed, spatial

20　trends differed between seasons, increasing progressively from the river mouth to the bay mouth in spring and autumn, and decreasing in winter. As tested by GAM analysis, the microplankton δ^{15}N values were stepwise elevated by environmental factors including temperature (GAM, $F = 5.0$, $P = 0.015$), salinity (GAM, $F = 5.0$, $P = 0.031$), ammonia (GAM, $F = 4.5$, $P = 0.031$), and nitrate (GAM, $F = 7.8$, $P = 0.010$). Similar to nanoplankton, regression analysis also showed that the microplankton δ^{15}N values increased significantly with increasing Chl a concentrations (GAM, $F = 4.2$, $P = 0.043$).

25　 Copepod δ^{15}N values ranged from 6.6 to 12.3‰ and were higher in summer than in other seasons (ANOVA, $F = 15.6$, $P < 0.001$). Generalized additive model analysis showed that the deviances of copepod δ^{13}C and δ^{15}N values explained by the GAMs were 92.7% and 76.9%, respectively (Table 3). Copepod δ^{13}C values changed significantly toward increasing salinity (GAM, $F = 7.9$, $P = 0.005$), for both the nanoplankton (GAM, $F = 6.2$, $P = 0.008$) and the microplankton (GAM, $F = 16.4$, $P < 0.001$; Fig. S1A–C). In contrast, temperature was the most important factor to explain the variability of copepod δ^{15}N values

30　(GAM, $F = 13.6$, $P < 0.001$; Fig. S1D). The microplankton δ^{15}N value was another important contributor to the variability of copepod δ^{15}N values (GAM, $F = 3.5$, $P = 0.034$; Fig. S1E), while nanoplankton δ^{15}N was not (GAM, $P > 0.05$). The Chl a concentration influenced the variability of copepod δ^{15}N values significantly (GAM, $F = 3.3$, $P = 0.047$; Fig. S1F).

3.3 Trophic positions of major groups

Multiple linear regression analyses to estimate mean isotopic values of different copepod groups (i.e., brackish calanoids, marine calanoids, and cyclopoids) from mixed copepod values (excluding harpacticoids) were all significant ($R^2 = 0.94$, $P < 0.001$ for $\delta^{13}C$; $R^2 = 0.78$, $P < 0.001$ for $\delta^{15}N$). The intercepts of the model indicating the errors of Eq. (1) and Eq. (2) were 1.1

5 ± 0.8‰ and 0.3 ± 0.8‰ for $\delta^{13}C$ and $\delta^{15}N$, respectively. The two calanoid groups displayed a close mean $\delta^{15}N$ value (around 9‰) but significantly different $\delta^{13}C$ values (-26.3 ± 1.5‰, -20.6 ± 1.6‰, and -20.1 ± 1.2‰ for brackish water calanoids and marine calanoids, respectively; Fig. 3A). Cyclopoids occupied a relative broad trophic niche based on a big coefficient of variation (41.6%), and the mean $\delta^{13}C$ value of cyclopoids (-31.0 ± 6.0‰) was even lower than those of brackish calanoids. The $\delta^{15}N$ values of the three major groups were all higher than the basal food resource (nanoplankton), and relatively higher

10 than microplankton with some overlap of error bar. The values of harpacticoids isolated from the winter (stations 2–9) and spring samples (stations 1) were measured directly. The mean $\delta^{15}N$ values of harpacticoids (6.9 ± 0.6‰) were lower than those of other copepods and microplankton, but relatively higher $\delta^{13}C$ value (-16.7 ± 1.4‰).

The multiple linear regression analysis performed for major copepod genera/species was also significant ($R^2 = 0.99$, $P < 0.001$ for $\delta^{13}C$; $R^2 = 0.88$, $P < 0.001$ for $\delta^{15}N$). The intercepts were 0.4 ± 0.7‰ and 0.8 ± 0.3‰ for $\delta^{13}C$ and $\delta^{15}N$, respectively. There

15 were two to three different trophic positions in the mixed copepod assemblages based on different $\delta^{15}N$ values (see patterns in Fig. 3B). The mean $\delta^{15}N$ values of *Corycaeus affinis* (13.7 ± 5.6‰), were the highest among taxa, followed by those of *Labidocera* (12.3 ± 3.9‰), *Tortanus* (12.3 ± 1.9‰), *Sinocalanus* (11.3 ± 1.7‰) and *Paracalanus* (11.0 ± 3.6‰). The mean values of *Acartia* (9.4 ± 2.6‰), *Calanus Sinicus* (9.0 ± 1.1‰), *Centropages* (8.1 ± 1.7‰) and *Eurytemora pacifica* (7.4 ± 2.5‰) indicated their trophic positions were relatively lower than those carnivorous species while they were higher than

20 nanoplankton. *Pseudodiaptomus* had a lowest value of $\delta^{15}N$ (5.3 ± 2.5‰) and it was even lower than microplankton and not much different to nanoplankton. Compared to of the two putative food resources (nanoplankton and microplankton), those brackish calanoid genera/species (*Pseudodiaptomus*, *E. pacifica, Paracalanus and Sinocalanus*) and *Corycaeus* had lower $\delta^{13}C$ than nanoplankton, while marine calanoid genera/species (*Tortanus*, *Labidocera, Calanus, Acartia* and *Centropages*) had higher values (Fig. 3B).

25 The trophic level in this study was defined as trophic position relative to nanoplankton, which was considered as the trophic baseline. Considering the TL of nanoplankton is 1, the TL value of microplankton was calculated to be 0.7 times higher than that of nanoplankton (Fig. 4). As a whole assemblage balanced from different feeding behaviors, as indicated by the standard errors, copepods occupied a 1.2 level higher TL than that of nanoplankton, indicating herbivory (here, herbivory means a trophic level of 2) on nanoplankton with slight omnivory (TL = 2–3) on other dietary sources. The TLs of three major calanoid

30 groups (marine calanoids and brackish calanoids) were similar to the bulk copepod assemblage with mean levels slightly higher than 2. The mean TL value of cyclopoids had apparently higher trophic level than calanoids. In contrast, the mean TL of harpacticoids was very low, reflected by their low $\delta^{15}N$ values.

Among calanoids, the mean TLs of *Eurytemora pacifica* (1 ± 0.5) and *Pseudodiaptomus* (1 ± 0.5) is indicative of their herbivorous and/or detritivorous characteristics. The mean TLs of *Calanus sinicus* (2.0 ± 0.6) and *Centropages* (1.6 ± 0.6) indicated they were primarily herbivorous*;* and those of *Acartia* and *Paracalanus* were slightly higher than 2 indicating they were primarily omnivorous feeding on both nanoplankton and microplankton. The levels of *Sinocalanus* (3.0 ± 0.7), *Tortanus*

5 and *Labidocera* were higher than 3.

Based on TLs, the mean ^{15}N enrichments of the copepod assemblage were estimated to be 3.4‰ and 1.7‰ for nanoplankton and microplankton, respectively (Fig. 5A, B). The enrichment values on nanoplankton for both marine and brackish calanoids, as well as for the genera of *Acartia* were close to the average value of the copepod assemblage. The trophic enrichment of *Calanus sinicus* on nanoplankton (3.0 ± 1.7‰) was slightly lower than averaged marine calanoids and total copepods, while

10 the enrichment on microplankton (1.7 ± 1.5‰) was similar. *Centropages* (1.9 ± 1.8‰) had much lower enrichment on nanoplankton compared to total copepods and marine calanoids. Four high TL genera *Tortanus*, *Labidocera*, *Sinocalanus* and *Corycaeus* had high enrichments > 6 on nanoplankton and > 3 on microplankton.

The ^{13}C enrichments for total copepods were on average 0.6‰ and 0.3‰ when feeding on nanoplankton and microplankton, respectively (Fig. 5C, D). Patterns were same with enrichments on ^{15}N.The four high TL genera *Tortanus*, *Labidocera*,

15 *Sinocalanus* and *Corycaeus* had high enrichments > 1.2 on nanoplankton and > 0.6 on microplankton. The enrichments of four herbivorous/omnivorous species increased from *Centropages, Calanus, and Acartia* to *Paracalanus*. In contrast, the brackish calanoid genera *Eurytemora* and *Pseudodiaptomus* had extremely low enrichments of both ^{15}N and ^{13}C.

3.4 Contribution of size-fractionated POM to copepod diets

The Bayesian mixing model calculations showed that the contributions of different sizes of POM to copepod diets varied

20 significantly with season (Student's *t*-test, *P* < 0.001 for all cases; Fig. 7). Size-selective feeding phenomena were particularly apparent in winter (Fig. S2A) and summer (Fig. S2C). Mean contributions of microplankton accounted for about two-thirds of their assimilated diets at all stations in winter and summer, and were almost equal to that of nanoplankton in spring and autumn (Fig. S2B, D). The proportions of the two size fractions of POM averaged from all four seasons contributing to copepod diets were also distinctly different at stations 2–5 and station 9 (Fig. S2). The mean contributions of microplankton to the copepod

25 diets increased gradually from the river mouth up to a peak (0.81 ± 0.11) at the middle part of the bay. Then, the proportion declined gradually to a trough (0.31 ± 0.18) at the deep-bay channel. The proportion then rebounded to a high level again at the bay mouth station.

Three major groups of copepods showed contrasting size-selective feeding behaviours (Fig. 6). Marine calanoids typically preferred feeding on larger particles, with a contributing proportion of 0.63 ± 0.03 (range: 0.50–0.71) for microplankton (Fig.

30 6A). Harpacticoids had a more apparent size-selective feeding behaviour preferring on microplankton (0.89 ± 0.10) and merely fed on nanoplankton (extremely low reliance of < 0.11; Fig. 6C). In contrast, brackish calanoids preferred feeding on nanoplankton (0.68 ± 0.05) to on microplankton (0.32 ± 0.05). For herbivorous/omnivorous copepod genera/species (e.g., *Acartia*, *C. sinicus*, *Centropages, E. pacifica*, *Paracalanus*, and *Pseudodiaptomus*), we tested their feeding preference on the

two size fractions of POM using the Bayesian mixing model (Fig. 7). *Acartia* and *Centropages* significantly preferred large to small particles (Student's *t*-test, $P < 0.001$)with a reliance of > 0.9 on microplankton (Fig. 7A, C),on the other hand, *C. sinicus* and *Paracalanus* apparently preferred small particles (Student's *t*-test, $P < 0.001$) (Fig. 7B, E).The two 'low trophic level' species/genus *Eurytemora pacifica* and *Pseudodiaptomus* had higher selecting on nanoplankton while there were high ranges of proportion of both potential food sources in diets(Fig. 7D, F). Based on TL showed above, we considered the four genera (*Labidocera*, *Sinocalanus*, *Tortanus* and *Corycaeus*) are carnivorous and able to predate other copepods. Thus, we tested the two fractions of POM and some herbivorous/omnivorous species/genera as potential food sources of them. The dietary compositions estimated by Bayesian mixing models showed slightly different among them (Fig. 8). Except *Sinocalnaus,* the other three carnivorous species all showed only negligible reliance on the two size fractions of POM. The marine calanoid genus *Labidocera* preferred predating on *Centropages* (0.35 ± 0.08*),* followed by harpacticoids (0.15 ± 0.10), *Acartia* (0.13 ± 0.09) and *Calanus* (0.10 ± 0.07) (Fig. 8A). On the contrary, besides of feeding on nanoplankton (0.23 ± 0.03), the brackish calanoid genus *Sinocalanus* also preferred predating on other brackish calanoids *Paracalanus* (0.37 ± 0.02), *Pseudodiaptomus* (0.15 ± 0.03) and followed by cyclopoids (0.09 ± 0.02) (Fig. 8B). *Tortanus* frequently co-occurred with many other copepods and its diet was composed of many different copepod species/genera without apparent selectivity (Fig.8C). The cyclopoid species *Corycaeus affinis* primarily predating on *Paracalanus* (0.67 ± 0.05) and *Pseudodiaptomus* (0.22 ± 0.06).

4 Discussion

4.1 Variability of δ^{13}C and δ^{15}N values of plankton with time and space

We found that seasonal variations and the spatial heterogeneity of copepod δ^{13}C and δ^{15}N values in Gwangyang Bay followed those of nanoplankton (POM < 20 μm) and microplankton (POM > 20 μm) (Figs 2 and 3). Based on the results of regression analyses, we found that the variability of copepod isotopic values was influenced by salinity (spatial variations), temperature (temporal variations), and isotopic values of food sources (both spatial and temporal variations; Fig. 3). In general, spatial variations were much more pronounced because of the effect of river input and thereby riverine carbon in different salinity regimes. More negative values of three plankton groups (nanoplankton, microplankton, and copepods) were measured near the river mouth, and then the values increased progressively to the mouth of the estuary, indicating an apparently decreasing effect of river runoff and thus the uptake of carbon derived from river-borne terrestrial organic matter. These results are consistent with other studies in estuarine environments (Cifuentes et al., 1988; Matson and Brinson, 1990; Thornton and McManus, 1994; Deegan and Garritt,1997; Fry, 2002). Such spatial distribution patterns have also been found for other primary producers such as seagrasses (reviewed by Hemminga and Mateo, 1996), macroalgae (Lee, 2000), as well as benthic microalgae (Kang et al., 2003), and the pattern will further propagate to consumers such as fish (Melville and Connolly, 2003; Herzka, 2005), oysters (Fry, 2002), mollusks (Antonio et al., 2010), and other benthic macro-invertebrates (Choy et al., 2008).

Seasonal successions of $\delta^{13}C$ values were also apparent, probably because of high river input in spring, elevated productivity in summer, and species successions in autumn. When the wet season started in spring and phytoplankton started to bloom, river input lowered the $\delta^{13}C$ values. The values increased again in summer because of the persistence of phytoplankton bloom (a low fractionation effect because of source limitation) and elevated productivity in summer. Although both river discharge and input of light carbon were low in autumn, the observed $\delta^{13}C$ values were low. This was probably because of the lack of a heavy carbon pool (a dissolved inorganic carbon pool in which the carbon was primarily composed of heavy ^{13}C) due to microbial respiration and species succession (Rau et al., 1990). During the post-bloom period in autumn, phytoplankton show low productivity and Chl a concentrations, with low abundance of diatoms but a dominance of flagellates (Baek et al., 2015). Flagellates are known to have more negative $\delta^{13}C$ values than those of diatoms arising from different fractionation effects (Gearing et al., 1984; Cifuentes et al., 1988; Rolff, 2000).

The $\delta^{15}N$ variability of three major plankton groups was relatively complex spatially. Seasonal pattern of nanoplankton $\delta^{15}N$ values, decreasing the values in summer to autumn, can well explained by the relationship between the $\delta^{15}N$ values and temperature, indicated by significant GAM analysis. Spatial trends in the nanoplankton $\delta^{15}N$ values can be explained by three distinct distribution patterns. The first pattern found in the river mouth area exemplifies a declining trend expected by mixing of freshwater planktonic materials, which grew up in water with high levels of dissolved inorganic nitrogen. The second pattern found in the middle part of the bay, in which nitrate inputs were low while the concentrations of ammonia increased (Kwon et al., 2004; own data not shown), characterizes an increase in $\delta^{15}N$ values in association with high Chl a concentrations. Fractionations by autotrophic assimilation and bacterial utilization were the most likely source of the ^{15}N-enriched ammonia in nutrient pools of the middle of the bay (Cifuentes et al., 1988). The elevated POM $\delta^{15}N$ values in the middle of the bay may be explained by ^{15}N-enriched ammonia remaining after algal uptake in the river mouth channel (Sato et al., 2006). The input of sewage-derived ^{15}N-enriched ammonia (domestic sewage and livestock waste) could contribute substantially and swamp the other subtle processes to increase $\delta^{15}N$ values of nanoplankton. The third distribution pattern represents declining $\delta^{15}N$ values toward the offshore bay mouth in association with a reduction in the supply of ^{15}N-enriched nutrients from terrestrial sewage. Furthermore, the fractionation effect of phytoplankton will be reduced when nutrients substantially decreased and phytoplankton would take up nitrogen with little fractionation and stored relatively light nitrogen isotope (Cifuentes et al., 1988; Fogel and Cifuentes, 1993; Granger et al., 2004). As indicated by GAM regression analyses between the distribution of nanoplankton $\delta^{15}N$ and environmental factors, significant increases in the nanoplankton $\delta^{15}N$ values depend on ammonia and Chl a, further supporting our explanation. The microplankton $\delta^{15}N$ values were stepwise elevated by environmental factors including temperature, salinity, ammonia and nitrate, indicated by significant results of GAM analysis (Table 2). Similar to nanoplankton, regression analysis also showed that the microplankton $\delta^{15}N$ values increased significantly with increasing Chl a concentrations (Table 2). One possible mechanism for this pattern is that higher phytoplankton abundance will result in a ^{15}N-enriched nutrient pool because of fractionation during nutrient assimilation (Kang et al., 2009). Nitrate was important for

microplankton, indicative of the role of diatoms (preferring nitrate) in controlling the variation in microplankton δ^{15}N values, whereas nanoflagellates (preferring ammonia) probably controlled the variation in nanoplankton δ^{15}N values.

As indicated by GAM analysis, the seasonality of copepod δ^{15}N values was primarily enhanced by temperature, which probably caused an elevated fractionation effect during the rapid assimilation of copepods. The lower explained deviance of δ^{15}N indicated reflects the food-web processes that affect δ^{15}N disproportionally and were not included in the GAM analysis. The regression relationship between larger plankton and copepods was significant, whereas the patterns were somewhat decoupled, as they were primarily observed in spring and autumn. This kind of decoupling has also been reported in the open ocean (Montoya et al., 2002), where the transfer of nitrogen from primary producers to zooplankton is weak. A time lag in zooplankton development might cause the mismatch of zooplankton to ^{15}N-enriched POM at the initial stage of nutrient supplies. Indeed, here we found that the high δ^{15}N values of copepods were primarily observed in summer, while the corresponding δ^{15}N values of POM started to increase from the winter, and phytoplankton blooming occurred in the spring.

4.2 Trophodynamics and trophic enrichments of copepods

The variability of copepod isotopic values in Gwangyang Bay suggests that the TLs of the copepod assemblage were highly dynamic. Because of different feeding behaviors and fractionation effects of copepods, the variability of the average community trophic position depends on the overall composition of species and is determined by the dominant species. Direct measurements of copepod isotopic values for species levels have been poorly conducted in the literature, although there are still clear patterns in existing reports. In the Southern Ocean copepods, the known carnivores *Euchaeta* and *Heterorhabdus* had high δ^{15}N values, while the acknowledged omnivores *Calanoides* and *Metridia* were intermediate in position, and *Rhincalanus* had the lowest values (Schmidt et al., 2003). A mesocosm study found that the δ^{15}N values were increasingly higher in the order *Temora < Pseudocalanus < Centropages*, suggesting an increase of carnivory in the same manner (Sommer et al., 2005). The trophic positions of primary consumers (*Oithona* and *Neocalanus*) and secondary consumers (*Pleuromamma* and *Euchaeta*) in the North Pacific Subtropical Gyre are estimated to be 2.1 and 2.9, respectively (Hannides et al., 2009). Furthermore, Kürten et al. (2011) reported that the relative trophic positions of zooplankton in the North Sea were high when the assemblage was mainly composed of *Sagitta* and *Calanus*, but low when the assemblage was dominated by *Pseudocalanus* and zoea larvae.

Our study has demonstrated the trophodynamics of estuarine copepods using multiple linear mixing model analysis based on the values of bulk samples and percentages in total biomass, by which the results of estimated δ^{13}C and δ^{15}N values were both significant ($P < 0.01$). The estimated δ^{13}C values varied greatly up to 10.9‰ among groups (from the lowest for cyclopoids to the highest for harpacticoids) and 14.2‰ among genera (from the lowest for *Paracalanus* to the highest for *Centropages*), respectively (Fig. 4). The estimated δ^{15}N values also varied somewhat up to 4.9‰ among groups, indicating one TL difference among groups if we consider 3–4‰ trophic enrichment of δ^{15}N between two adjacent TLs (Post, 2002; Michener and Kaufman, 2007). The trophic enrichments calculated by the differences from the basal food sources indicate that the overall enrichments

14

of copepods were around 3.4‰ and 1.7‰ from nanoplankton and microplankton, respectively (Fig. 6). Our estimation shows that both marine calanoids and brackish water calanoids overall occupy a similar trophic niche (i.e., similar mean $\delta^{15}N$ values), but have contrasting food sources (i.e., different $\delta^{13}C$ values; Fig. 4A). The isotopic values of calanoid copepods indicate a mixture of different genera including both high and low $\delta^{15}N$ values. For example, marine calanoids were mixed by high $\delta^{15}N$ genera (*Tortanus* and *Labidocera*) and low $\delta^{15}N$ genera (*Acartia, Calanus, Centropages*) and moderate $\delta^{15}N$ genera (*Paracalanus* and *Acartia*). Brackish types were mixed by high $\delta^{15}N$ genera (*Sinocalanus*) and low $\delta^{15}N$ genera (*Eurytemora* and *Pseudodiaptomus*). Consequently, the two major calanoids groups (marine and brackish water types) as well as the mixture of all copepod groups were estimated to be on average one TL higher than the nanoplankton base (Fig. 4). However, we do not necessarily conclude that they are herbivores because the nanoplankton studied here represent POM with a size range of 2–20 μm, which may include ciliates, heterotrophic nanoflagellates, and heterotrophic dinoflagellates. Instead, all assemblages mentioned above might be omnivorous with varying levels of relative trophic positions depending on dominant species.

Among calanoids, brackish water species had significantly lower $\delta^{13}C$ values than marine species, indicative of an apparent effect of riverine carbon sources on brackish species through the food web (Fig. 3). These results were consistent with the distribution pattern that most brackish species occurred or dominant in the upper part of Gwangyang Bay. *Sinocalanus tenellus* had contrasting TL value to those of *Pseudodiaptomus* and *Eurytemora* (Fig. 4B), indicating a mixture of brackish water calanoids being close to omnivory with a broad feeding size spectrum. However, as *Sinocalanus* and *Pseudodiaptomus* s were dominant in different seasons (Table 1), the TLs of the copepod assemblage at a specific condition will become relatively carnivorous (*Sinocalanus* dominating) or omnivorous (*Pseudodiaptomus* and *Paracalanus parvus* dominating). *P. parvus* is an important small species (body length ≤1mm) that is widely distributed in coastal and estuarine waters worldwide (Turner, 2004). Our results showed that, similar to other brackish water calanoids, this species was greatly influenced by ^{13}C-depleted dietary sources, dominating both brackish stations in autumn and saline stations in winter (Table 1). This result indicates that *Paracalanus* was well adapted to fluctuating estuarine environments by feeding on prey originating from freshwater or prey that depends on riverine carbon sources. *Acartia,* one of the commonest genus in Gwangyang Bay throughout the year (Table 1), included both marine types (*A. hudsonica* and *A. Omorii*) and brackish types *(A. ohtsukai*, and *A. erythraea*) based on literature (Table S1). Marine types of *Acartia* primarily occurred or dominated during the winter and spring, while brackish type dominated during the summer. Overall the genus of *Acartia* had higher $\delta^{13}C$ values than those of *Paracalanus*, suggesting their different food sources. *Acartia* is also a widely distributed genus, with a switching feeding behaviour in response to the status of food composition (Kiøboe et al., 1996; Rollwagen-Bollens and Penry, 2003; Chen et al., 2013). The isotopic values of *Acartia* were similar to those the assemblage of marine calanoids, indicating that this genus is omnivorous, as typical of marine calanoids. The marine calanoids species *C. sinicus* had a close trophic niche to total marine calanoids based on similar $\delta^{15}N$ value and trophic level (Fig. 4), 1 TL higher than nanoplankton suggesting that this species is a typical marine herbivore relative to nanoplankton. Conversely, two other marine calanoid genera, *Tortanus* (*T. dextrilobatus* and *T. forcipatus*) and *Labidocera* (*L. euchaeta* and *L. rotunda*), were primarily carnivorous as indicated by their $\delta^{15}N$ values (Figs. 3B and 4). These

estimated results are consistent with the former experimental tests and field investigations (Ambler and Frost, 1974; Landry, 1978; Conley and Turner, 1985; Hooff and Bollens, 2004). Cyclopoids (primarily *Corycaeus affinis*) dominated copepod assemblages in spring and autumn at the middle part and deep-bay channel of the bay (Table 1). Our data reveal that *Corycaeus* was primarily carnivorous, being 2 TLs higher than nanoplankton (Fig. 4) and prefers feeding on ^{13}C-depleted dietary sources (Fig. 3). This result is consistent with previous reports that the *Corycaeus* genus is carnivorous (Gophen and Harris, 1981; Landry et al., 1985; Turner, 1984).

Isotopic values of microplankton indicate that they are roughly a half TL value higher than nanoplankton. Considering that the sizes of most ciliates and heterotrophic dinoflagellates primarily fall within this size spectrum (20–200 µm), this result suggests an omnivorous trend among the mixed microplankton groups. Similarly, although measured only in winter samples, the benthic copepod group harpacticoids, represented by the species *Euterpina* sp.*,* also differed from calanoids and cyclopoids with low δ^{15}N values. The TL of harpacticoids estimated from this approach was somewhat misleading because of their unexpectedly low δ^{15}N values, which probably reflect feeding on detritus or dead organisms that are depleted in ^{15}N (Sautour and Castel, 1993).

4.3 Selective feeding of copepods

Feeding preferences of different groups or genera on two size fractions of POM are of particular importance to explain seasonal and spatial patterns of community trophic niches, and in turn will predict the impacts of the grazer community on lower TLs including phytoplankton and microzooplankton. Because not all possible food sources, such as bacteria, picoplankton, fecal pellets, and dead detritus, were investigated, our Bayesian mixing model calculations might have led to some biased results. Nevertheless, the model results might provide an estimation on what size fractions of dietary sources the grazer community ingest and assimilate. In general, our results highlight that the copepod assemblages have size-selective feeding behaviors, and that these vary with season (Fig. S2) and space (Fig. S3). The feeding selectivity of the bulk copepod assemblage was a balance of ingestion among different groups. The whole copepod assemblage assimilated two-thirds of its food requirement from microplankton in winter and summer, but they fed nearly equally on both size fractions of POM in spring and autumn (Fig. S2). Our results suggest that groups that preferred large-sized prey played a more important role in total assemblage of copepods in winter and summer, during which the assemblage were primarily dominated by marine calanoids (Table 1). On the other hand, in the spring and autumn when the assemblage was primarily dominated by carnivorous species (*Corycaeus*, *Tortanu*s) and dominated by both *Paracalanus* (our result suggested this genus was an omnivorous species and the size-selectivity was less pronounced preferring small-sized particle) and *Acartia* (preferring large-sized particle), the assemblage overall didn't show an apparent size-selectivity.

Based on the model results for major copepod groups and genera, marine calanoids preferred feeding on large particles (Figs. 6A and 7A) Such a size-selective feeding preference has been widely reported in many field investigations (Liu et al., 2005a; Jang et al., 2010; Chen et al., 2017). On the contrary, brackish calanoids as a group preferred feeding on small-sized plankton. These results were not well reported in literature. Among calanoids, *Acartia and Paracalanus* both contain marine species and

brackish species. Our model results showed that *Acartia* preferred feeding on large-sized plankton, while *Paracalanus* was contrastingly different. *Acartia*, well studied in literature, are reported to prefer feeding on phytoplankton larger than 20 μm in the coastal water adjacent to the present study area (Jang et al., 2010). Besides, due to nutritional requirements, *Acartia* were reported that they preferred predating microzooplankton such as ciliates and heterotrophic dinoflagellates (Wiadnyana and

5   Rassoulzadegan, 1989; Chen et al., 2013). On the other hand, another dominant calanoid genus, *Paracalanus*, preferred feeding on nanoplankton (Fig. 7E), suggesting that the feeding efficiency, with which the grazers' feeding appendage to retain particles, differs between these two genera. Because of such different feeding preferences, they dominated in different stations or seasons with differing food conditions (Table 1) and frequently co-occurred with little overlap of preferred food particle sizes. Besides, low $\delta^{13}C$ value of *P. parvus* indicated that this wildly distributed species preferred feeding on particles flourished from

10   terrestrial carbon.

Although *C. sinicus* was not dominant in abundance, this species contributes a great amount in biomass due to large body size (Table S1). Similar to *Paracalanus*, *C. Sinicus* preferred feeding on small-sized particles, while the difference is that the relatively high $\delta^{13}C$ value of *C. Sinicus* indicated that this species preferred prey originated from offshore areas. The result is consistent with reports that *C. Sinicus* is a dominant species in Yellow Sea and East China Sea (the offshore shelf waters of

15   this study estuary) (Uye, 2000; Liu et al., 2003). Another marine calanoid genus similar to *Acartia, Centropages* (*C. abdominalis* and *dorsispinatus*) apparently preferred feeding on large-sized plankton (this study and Wiadnyana and Rassoulzadegan, 1989). For other two marine calanoid genera —*Labidocera* (*L. rotunda* and *L. euchaeta*) and *Tortanus* (*T. dextrilobatus* and *T. forcipatus*) — feeding on two size fractions of POM did not occur, based on no contribution of the two size fractions of POM to their diets (Fig. 8A, C). Model results indicated that *Labidocera and Tortanus* were carnivorous

20   genera, consistent with many reports (Landry, 1978; Mullin, 1979; Turner, 1984; Uye, 1994; Hooff and Bollens, 2004). Our result also showed that *Labidocera* had an apparent selectivity in predating their prey, preferring marine calanoids (*Acartia, Calanus* and *Centropages*) and harpacticoids. This feeding selectivity was consistent with the distribution of this species. It never distributed in river stations (stations 1–3) (Table S2) and even dominated at station 7 during the summer (Table 1). Differently, *Tortanus* didn't show selectivity among different prey (Fig. 8C) and thus this genus occurred frequently in

25   different stations (Table S2).

The model results indicated that the size selectivity of brackish water calanoids such as *Pseudodiaptomus* and *Eurytemora* was also apparently for nanoplankton similar to *Paracalanus* (Fig.7 D, F). To our knowledge, the feeding habit of *Pseudodiaptomus* is unknown in the current literature, whereas some field studies suggest that estuarine *Pseudodiaptomus* flourishes by feeding on small phytoplankton cells (< 20 μm) (Froneman, 2004), consistent with the present results. Incorporating the results of low

30    $\delta^{13}C$ values of *Pseudodiaptomus* and *Eurytemora*, we believe that these two genera were able to feed on those prey with small sizes (2–20 μm) and low $\delta^{13}C$ from originated from terrestrial sources, whereas low trophic position and trophic enrichments indicated that these two genera may ingest prey with extremely low $\delta^{15}N$ compared to nanoplankton (e.g., detritus). The detritus with low $\delta^{15}N$ may contribute to the balance the $\delta^{15}N$ of *Pseudodiaptomus* and *Eurytemora*, and thus, they may act as

17

detritivores besides of herbivores. Another brackish calanoid species —*Sinocalanus tenellus* were more diverse in feeding selectivity (Fig. 8B). It can act as a suspension feeder preferring small-sized plankton as well as a raptorial feeder preferring predating other brackish calanoids and cyclopoids. This species was even reported as a cannibalistic feeder in estuary (Hada and Uye, 1991).

5 In contrast to both marine calanoids and brackish water calanoids, the cyclopoid species *Corycaeus affinis* was a carnivorous species preferring predating on two brackish species —*Paracalanus and Pseudodiptomus* (Fig. 8D). This species is a widely distributed in all the world's oceans (Turner, 2004) and also frequently dominate in copepod assemblages in spring and autumn in Gwangyang Bay (Table 1). Although the isotopic data for harpacticoid copepods were limited to only one season, we still obtained a clear feeding selectivity pattern based on the Bayesian mixing model (Fig. 7C). Harpacticoids in winter preferred

10 microplankton to nanoplankton if benthic food sources were not considered. Their feeding selectivity contributed to the overall feeding preference of total copepods in this season.

5 Conclusions

Here we have demonstrated the temporal and spatial variability of stable isotope ratios of copepods, which was determined by the isotopic values of two size fractions of POM, and strongly influenced by salinity (spatiality) and temperature (temporality).

15 Such characteristic is a key in understanding the biogeochemical cycles of carbon and nitrogen in Gwangyang Bay. We further used a simple linear mixing model and a Bayesian mixing model to extrapolate from the information derived from the isotopic analysis of bulk copepod samples. The model results were robust and allowed the estimation of the relative TLs and trophic enrichment (fractionation effect) of different groups and dominant genera of copepods, as well as their diet compositions. Temporal and spatial patterns of copepod isotopic traits were further explained by size selectivity on plankton size fractions,

20 as well as the feeding preference of dominant species. Based on such relative trophic positions and feeding preference, we can depict a simple energy flow of the Gwangyang Bay planktonic food web: from primary producers (nanoplankton) and a mixture of primary producers and herbivores (microplankton) through omnivores (represented by *Calanus*, *Centropages*, *Acartia*, and *Paracalanus*) and detrivores (represented by *Pseudodiptomus* and *Eurytemora*) to carnivores (dominated by *Corycaeu, Tortanus*, *Labidocera*, and *Sinocalanus*) (see a simplified energy flow, Fig. 9).

25

References

Ambler, J. W. and Frost, B. W.: The feeding behavior of a predatory planktonic copepod, *Torlanus discaudatus*. Limnol. Oceanogr., 19, 446–451, 1974.

Anger, K.: The Biology of Decapod Crustacean Larvae, Crustacean Issues 14, AA Balkema Publishers, Rotterdam, Netherlands, 2001.

Antonio, E. S., Kasai, A., Ueno, M., Kurikawa, Y., Tsuchiya, K., Toyohara, H., Inshihi, Y., Yokoyama, H., and Yamashita, Y.: Consumption of terrestrial organic matter by estuarine molluscs determined by analysis of their stable isotopes and cellulase activity. Estuar. Coast. Shelf Sci., 86, 401–407, 2010.

Baek, S. H., Kim, D., Son, M., Yun, S. M., and Kim, Y.O.: Seasonal distribution of phytoplankton assemblages and nutrient-enriched bioassays as indicators of nutrient limitation of phytoplankton growth in Gwangyang Bay, Korea. Estuar. Coast. Shelf Sci., 163, 265–278, 2015.

Berk, S. G., Brownlee, D. C., Heinle, D. R., Kling, H. J., and Colwell, R. R.: Ciliates as a food source for marine planktonic copepods. Microb. Ecol., 4, 27–40, 1977.

Calbet, A. and Saiz, E.: The ciliate-copepod link in marine ecosystems. Aquatic Microb. Ecol., 38, 157–167, 2005.

Checkley D. M. and Entzeroth, L. C.: Elemental and isotopic fractionation of carbon and nitrogen by marine, planktonic copepods and implications to the marine nitrogen cycle. J. Plankton Res., 7, 553–568, 1985.

Checkley, D. M. and Miller, C. A.: Nitrogen isotope fractionation by oceanic zooplankton. Deep-Sea Res. Part I, 36, 1449–1456, 1989.

Chen, M. and Liu, H.: Experimental simulation of trophic interactions among omnivorous copepods, heterotrophic dinoflagellates and diatoms. J. Exp. Mar. Biol. Ecol., 403, 65–74, 2011.

Chen, M., Liu, H. and Li, H.: Effect of mesozooplankton feeding selectivity on the dynamics of algae in the presence of intermediate grazers a laboratory simulation. Mar. Ecol. Prog. Ser., 486, 47–58, 2013.

Choy, E. J., An, S., and Kang, C. K.: Pathways of organic matter through food webs of diverse habitats in the regulated Nakdong River estuary (Korea). Estuar. Coast. Shelf Sci., 78, 215–226, 2008.

Cifuentes, L. A., Sharp, J. H., and Fogel, M. L.: Stable carbon and nitrogen isotope biogeochemistry in the Delaware estuary. Limnol. Oceanogr., 33, 1102–1115, 1988.

Conley, W. J. and Turner, J. T.: Omnivory by the coastal marine copepods *Centropages hamatus* and *Labidocera aestiva*. Mar. Ecol. Prog. Ser., 241, 113–120, 1985.

Deegan, L. A. and Garritt, R. H.: Evidence for spatial variability in estuarine food webs. Mar. Ecol. Prog. Ser., 147, 31–47, 1997.

Fessenden, L. and Cowles, T. J.: Copepod predation on phagotrophic ciliates in Oregon coastal waters. Mar. Ecol. Prog. Ser., 107, 103–111, 1994.

Fogel, M. L. and Cifuentes, L. A.: Isotope fractionation during primary production, in: Organic Geochemistry, Engel, M. H. and Macko, S. A. eds., Plenum Press, New York, 73–98, 1993.

5   Francis, T. B., Schindler, D. E., Holtgrieve, G. W., Larson, E. R., Scheuerell, M. D., Semmens, B. X., and Ward, E. J.: Habitat structure determines resource use by zooplankton in temperate lakes. *Ecol. Let.*, 14, 364–372, 2011.

Froneman, P. W.: In situ feeding rates of the copepods, *Pseudodiaptomus hessei* and *Acartia longipatella*, in a temperate, temporarily open/closed Eastern Cape estuary. S. Afr. J. Sci., 100, 577–583, 2004.

Fry, B.: Conservative mixing of stable isotopes across estuarine salinity gradients: a conceptual framework for monitoring
10   watershed influences on downstream fisheries production. Estuar. Coast., 25, 264–271, 2002.

Fry, B.: Stable Isotope Ecology. Springer Science & Business Media, New York, USA, 2007.

Gearing, J. N., Gearing, P. J., Rudnick, D. T., Requejo, A. G., and Hutchins, M. J.: Isotopic variability of organic carbon in a phytoplankton-based, temperate estuary. Geochim. Cosmoch. Acta, 48, 1089–1098, 1984.

Gifford, S. M., Rollwagen-Bollens, G., and Bollens, S. M.: Mesozooplankton omnivory in the upper San Francisco Estuary.
15   Mar. Ecol. Prog. Ser., 348, 33–46, 2007.

Gophen, M. and Harris, R. P.: Visual predation by a marine cyclopoid copepod, *Corycaeus anglicus*. J. Mar.Biol. Ass. UK, 61, 391–399, 1981.

Graeve, M., Hagen, W., and Kattner, G.: Herbivorous or omnivorous? On the significance of lipid compositions as trophic markers in Antarctic copepods. Deep-Sea Res. Part I, 41, 915–924, 1994.

20   Granger, J., Sigman, D. M., Needoba, J. A., and Harrison, P. J.: Coupled nitrogen and oxygen isotope fractionation of nitrate during assimilation by cultures of marine phytoplankton. Limnol. Oceanogr., 49, 1763–1773, 2004.

Grey, J., Jones, R. I., and Sleep, D.: Seasonal changes in the importance of the source of organic matter to the diet of zooplankton in Loch Ness, as indicated by stable isotope analysis. Limnol. Oceanogr., 46, 505–513, 2001.

Hada, A. and Uye, S.: Cannibalistic feeding behavior of the brackish-water copepod *Sinocalanus tenellus*. J. Plankton. Res.,
25   13, 155–166, 1991.

Hannides, C., Popp, B. N., Landry, M. R., and Graham, B. S.: Quantification of zooplankton trophic position in the North Pacific Subtropical Gyre using stable nitrogen isotopes. Limnol. Oceanogr., 54, 50–61, 2009.

Hemminga, M. A. and Mateo, M. A.: Stable carbon isotopes in seagrasses: variability in ratios and use in ecological studies. Mar. Ecol. Prog. Ser., 140, 285–298, 1996.

30   Herzka, S. Z.: Assessing connectivity of estuarine fishes based on stable isotope ratio analysis. Estuar. Coast. Shelf Sci., 64, 58–69, 2005.

Hooff, R. C. and Bollens, S. M.: Functional response and potential predatory impact of *Tortanus dextrilobatus*, a carnivorous copepod recently introduced to the San Francisco Estuary. Mar. Ecol. Prog. Ser., 277, 167–179, 2004.

Jang, M. -C., Shin, K., Lee, T., and Noh, I.: Feeding selectivity of calanoid copepods on phytoplankton in Jangmok Bay, South

Coast of Korea. Ocean Sci. J., 45.101–111, 2010.

Jeffrey, S. W.: Application of pigment methods to oceanography, in: Phytoplankton Pigments in Oceanography: Guidelines to Modern Methods, Jeffery, S. W., Mantoura, R. F. C., and Wright, S. W. eds., UNESCO Publishing, Paris, France, 127–166, 1997.

5 Kang, C. K., Kim, J. B., Lee, K. S., Kim, J. B., Lee, P. Y., and Hong, J. S.: Trophic importance of benthic microalgae to macrozoobenthos in coastal bay systems in Korea: dual stable C and N isotope analyses. Mar. Ecol. Prog. Ser., 259, 79–92, 2003.

Kang, C. K., Choy, E. J., Hur, Y. B., and Myeong, J. I.: Isotopic evidence of particle size-dependent food partitioning in cocultured sea squirt *Halocynthia roretzi* and Pacific oyster *Crassostrea gigas*. Aquat. Biol., 6, 289–302, 2009.

10 Kim, B. J., Ro, Y. J., Jung, K. Y., and Park, K. S.: Numerical modeling of circulation characteristics in the Kwangyang Bay estuarine system. J. Korean Soc. Coast. Ocean Eng. 26: 253–266, 2014.

Kim, S. Y., Moon, C. H., Cho, H. J., and Lim, D. I.: Dinoflagellate cysts in coastal sediments as indicators of eutrophication: a case of Gwangyang Bay, South Sea of Korea. Estuar. Coast., 32, 1225–233, 2009.

Kiørboe, T., Saiz, E., and Viitasalo, M.: Prey switching behaviour in the planktonic copepod *Acartia tonsa*. Mar. Ecol. Prog. 15 Ser., 143, 65–75, 1996.

Kürten, B., Painting, S. J., Struck, U., Polunin, N. V., and Middelburg, J. J.: Tracking seasonal changes in North Sea zooplankton trophic dynamics using stable isotopes. Biogeochemistry, 113, 1–21, 2013.

Kwak, J. H., Han, E., Lee, S. H., Park, H. J., Kim, K. R., and Kang, C. K.: A consistent structure of phytoplankton communities across the warm–cold regions of the water mass on a meridional transect in the East/Japan Sea. Deep–Sea Res Part II, 143, 20 36–44, 2017.

Kwon, K. Y., Moon, C. H., Kang, C. K., and Kim, Y. N.: Distribution of particulate organic matters along the salinity gradients in the Seomjin River estuary. Korean J. Fish. Aquat. Sci., 35, 86–96, 2002.

Kwon, K. Y., Moon, C. H., Lee, J. S., Yang, S. R., Park, M. O., and Lee, P. Y.: Estuarine behavior and flux of nutrients in the Seomjin River estuary. The Sea J. Korean Soc. Oceanogr., 9, 153–163, 2004.

25 Landry, M. R.: Predatory feeding behavior of a marine copepod, *Labidocera trispinosa*. Limnol. Oceanogr., 23, 1103–1113, 1978.

Landry, M. R., Lehner-Fournier, J. M., and Fagerness, V. L.: Predatory feeding behavior of the marine cyclopoid copepod *Corycaeus anglicus*. Mar. Biol., 85, 163–169, 1985.

Layman, C. A., Araujo, M. S., Boucek, R., Hammerschlag-Peyer, C. M., Harrison, E., Jud, Z. R., and Post, D. M.: Applying 30 stable isotopes to examine food-web structure: an overview of analytical tools. Biol. Rev., 87, 545–562, 2012.

Lee, S. Y.: Carbon dynamics of Deep Bay, eastern Pearl River estuary, China. II: Trophic relationship based on carbon-and nitrogen-stable isotopes. Mar. Ecol. Prog. Ser., 205, 1–10, 2000.

Lee, Y. W., Park, M. O., Kim, Y. S., Kim, S. S., and Kang, C. K.: Application of photosynthetic pigment analysis using a HPLC and CHEMTAX program to studies of/ phytoplankton community composition. The Sea J. Korean Soc. Oceanogr., 16,

117–124, 2011.

Liu, H., Dagg, M. J., and Strom, S.: Grazing by the calanoid copepod *Neocalanus cristatus* on the microbial food web in the coastal Gulf of Alaska. J. Plankton Res., 27, 647–662, 2005a.

Liu, H., Dagg, M., Wu, C., and Chiang, K.: Mesozooplankton consumption of microplankton in the Mississippi River plume, with special emphasis on planktonic ciliates. Mar. Ecol. Prog. Ser., 286, 133–144, 2005b.

Liu, G.M., Sun, J., Wang, H., Zhang, Y., Yang, B., and Ji, B.: Abundance of *Calanus sinicu*s across the tidal front in the Yellow Sea, China. Fish. Oceanogr., 12, 291–298, 2003.

Matson, E. A. and Brinson, M. M.: Stable carbon isotopes and the C: N ratio in the estuaries of the Pamlico and Neuse Rivers. North Carolina. Limnol. Oceanogr., 35, 1290–1300, 1990.

McClelland, J. W. and Montoya, J. P.: Trophic relationships and the nitrogen isotopic composition of amino acids in plankton. Ecology, 83, 2173–2180, 2002.

Melville, A. J. and Connolly, R. M.: Spatial analysis of stable isotope data to determine primary sources of nutrition for fish. Oecologia, 136, 499–507, 2003.

Michener, R. H. and Kaufman, L.: Stable isotope ratios as tracers in marine food webs: an update. Stable Isotopes in Ecology and Environmental Science, 2, 238–282, 2007.

Montoya, J. P., Carpenter, E. J., and Capone, D. G.: Nitrogen fixation and nitrogen isotope abundances in zooplankton of the oligotrophic North Atlantic. Limnol. Oceanogr., 47, 1617–1628, 2002.

Montoya, J. P., Horrigan, S. G., and McCarthy, J. J.: Rapid, storm-induced changes in the natural abundance of ^{15}N in a planktonic ecosystem, Chesapeake Bay, USA. Geochim. Cosmochim. Acta, 55, 3627–3638, 1991.

Moore, J. W. and Semmens, B. X.: Incorporating uncertainty and prior information into stable isotope mixing models. Ecol. Let., 11, 470–480, 2008.

Mullin, M. M.: Differential predation by the carnivorous marine copepod *Tortanus discautus*. Limnol. Oceanogr, 24, 774–777, 1979.

Needoba, J. A., Waser, N. A., Harrison, P. J., and Calvert, S. E.: Nitrogen isotope fractionation in 12 species of marine phytoplankton during growth on nitrate. Mar. Ecol. Prog. Ser., 255, 81–91, 2003.

Nejstgaard, J. C., Naustvoll, L. J., and Sazhin, A.: Correcting for underestimation of microzooplankton grazing in bottle incubation experiments with mesozooplankton. Mar. Ecol. Prog. Ser., 221, 59–75, 2001.

Park, E. O., Suh, H. L., and Soh, H. Y.: Spatio-temporal distribution of *Acartia* (Copepoda: Calanoida) species along a salinity gradient in the Seomjin River estuary, South Korea. J. Nat. Hist., 49, 2799–2812, 2015.

Park, H. J., Han, E., Lee, Y. J., and Kang, C. K.: Trophic linkage of a temperate intertidal macrobenthic food web under opportunistic macroalgal blooms: A stable isotope approach. Mar. pollut. Bull., 111, 86–94, 2016.

Parnell, A. C., Inger, R., Bearhop, S., and Jackson, A. L.: Source partitioning using stable isotopes: coping with too much variation. PloS One, 5, e9672, 2010.

Parnell, A. C., Phillips, D. L., Bearhop, S., Semmens, B. X., Ward, E. J., Moore, J. W., Jackson, A.L., Grey, J., Kelly, D. J.,

and Inger, R.: Bayesian stable isotope mixing models. Environmetrics, 24, 387–399, 2013.

Phillips, D. L. and Gregg, J. W.: Source partitioning using stable isotopes: coping with too many sources. Oecologia, 136, 261–269, 2003

Phillips, D. L. and Koch, P. L.: Incorporating concentration dependence in stable isotope mixing models. Oecologia, 130, 114–125, 2002.

Post, D. M.: Using stable isotopes to estimate trophic position: models, methods, and assumptions. Ecology, 83, 703–718, 2002.

Rau, G.H., Teyssie, J.L., Rassoulzadegan, F., and Fowler, S.W.: $^{13}C/^{12}C$ and $^{15}N/^{14}N$ variations among size-fractionated marine particles: implications for their origin and trophic relationships. Mar. Ecol. Prog. Ser., 59, 33–38, 1990.

Rolff, C.: Seasonal variation in $\delta^{13}C$ and $\delta^{15}N$ of size-fractionated plankton at a coastal station in the northern Baltic proper. Mar. Ecol. Prog. Ser., 203, 47–65, 2000.

Rollwagen-Bollens, G. C. and Penry, D. L.: Feeding dynamics of *Acartia* spp. copepods in a large, temperate estuary (San Francisco Bay, CA). Mar. Ecol. Prog. Ser., 257, 139–158, 2003.

Sato, T., Miyajima, T., Ogawa, H., Umezawa, Y., and Koike, I.: Temporal variability of stable carbon and nitrogen isotopic composition of size-fractionated particulate organic matter in the hypertrophic Sumida River Estuary of Tokyo Bay, Japan. Estuar. Coast. Shelf Sci., 68, 245–258, 2006.

Sautour, B. and Castel, J.: Feeding behaviour of the coastal copepod *Euterpina acutifrons* on small particles. Cah. Biol. Mar., 34, 239-251, 1993

Schmidt, K., Atkinson, A., Stübing, D., McClelland, J. W., Montoya, J. P., and Voss, M.: Trophic relationships among Southern Ocean copepods and krill: some uses and limitations of a stable isotope approach. Limnol. Oceanogr., 48, 277–289, 2003.

Sell, A. F., van Keuren, D., and Madin, L. P.: Predation by omnivorous copepods on early developmental stages of *Calanus finmarchicus* and *Pseudocalanus* spp. Limnol. Oceanogr., 46, 953–959, 2001.

Sommer, F., Saage, A., Santer, B., Hansen, T., and Sommer, U.: Linking foraging strategies of marine calanoid copepods to patterns of nitrogen stable isotope signatures in a mesocosm study. Mar. Ecol. Prog. Ser., 286, 99–106, 2005.

Sommer, U. and Sommer, F.: Cladocerans versus copepods: the cause of contrasting top–down controls on freshwater and marine phytoplankton. Oecologia, 147, 183–194, 2006.

Stibor, H., Vadstein, O., Diehl, S., Gelzleichter, A., Hansen, T., Hantzsche, F., Katechakis, A., Lippert, B., Løseth, K., Peters, C., Roederer, W., Sandow, M., Sundt-Hansen, L., and Olsen, Y.: Copepods act as a switch between alternative trophic cascades in marine pelagic food webs. Ecol. Let., 7, 321–328, 2004.

Tamelander, T., Søreide, J. E., Hop, H., and Carroll, M. L.: Fractionation of stable isotopes in the Arctic marine copepod *Calanus glacialis*: effects on the isotopic composition of marine particulate organic matter. J. Exp. Mar. Biol. Ecol., 333, 231–240, 2006.

Thornton, S. F. and McManus, J.: Application of organic carbon and nitrogen stable isotope and C/N ratios as source indicators

of organic matter provenance in estuarine systems: evidence from the Tay Estuary, Scotland. Estuar. Coast. Shelf Sci., 38, 219–233, 1994.

Turner, J. T.: Zooplankton feeding ecology: contents of fecal pellets of the copepods *Acartia tonsa* and *Labidocera aestiva* from continental shelf waters near the mouth of the Mississippi River. Mar. Ecol., 5, 265–282, 1984.

5   Turner, J. T.: Zooplankton feeding ecology: contents of fecal pellets of the cyclopoid copepods *Oncaea venusta*, *Corycaeus amazonicus*, *Oithona plumifera*, and *O. simplex* from the northern Gulf of Mexico. Mar. Ecol., 7, 289–302, 1986.

Turner, J. T.: The importance of small planktonic copepods and their roles in pelagic marine food webs. Zool. Stud., 43, 255–266, 2004.

Uye, S. Why does *Calanus sinicus* prosper in the shelf ecosystem of the Northwest Pacific Ocean? ICES J. Mar. Sci, 57, 1850–
10   1855, 2000.

Vadstein, O., Stibor, H., Lippert, B., Løseth, K., Roederer, W., Sundt-Hansen, L., and Olsen, Y.: Moderate increase in the biomass of omnivorous copepods may ease grazing control of planktonic algae. Mar. Ecol. Prog. Ser., 270, 199–207, 2004.

Ward, E. J., Semmens, B. X., and Schindler, D. E.: Including source uncertainty and prior information in the analysis of stable isotope mixing models. Environ. Sci. Tech., 44, 4645–4650, 2010.

15   Waser, N. A. D., Harrison, P. J., Nielsen, B., Calvert, S. E., and Turpin, D. H.: Nitrogen isotope fractionation during the uptake and assimilation of nitrate, nitrite, ammonium, and urea by a marine diatom. Limnol. Oceanogr., 43, 215–224, 1998.

Wiadnyana, N.N. and Rassoulzadegan, F.: Selective feeding of *Acartia clause* and *Centropages typicus* on microzooplankton. Mar. Ecol. Prog. Ser., 53, 37–45, 1989.

Wood, S. and Wood, M. S.: Package ″mgcv″. R Package Version 1.7–29, 2015.

20   Zapata, M., Rodríguez, F., and Garrido, J. L.: Separation of chlorophylls and carotenoids from marine phytoplankton: a new HPLC method using a reversed phase C8 column and pyridine-containing mobile phases. Mar. Ecol. Prog. Ser., 195, 29–45, 2000.

Zöllner, E., Hoppe, H. G., Sommer, U., and Jürgens, K.: Effect of zooplankton-mediated trophic cascades on marine microbial food web components (bacteria, nanoflagellates, ciliates). Limnol. Oceanogr., 54, 262–275, 2009.

25

Table 1: Seasonal variations in basic environmental factors, including temperature (T), salinity (S), and chlorophyll *a* (Chl *a*), copepod abundance, and dominant species and the percentage (%) of dominant species in total copepods at the 9 stations in the Gwangyang Bay system.

Seasons	Stations	T (°C)	S (psu)	Chl *a* (μg l^{-1})	Copepod Abundance (ind. m^{-3})	Dominant species	% of dominant species
Winter February 2015	1	7.4	1.4	1.2	65	*Acartia hudsonica*	45
	2	9.1	8.0	2.2	551	*Acartia hudsonica*	89
	3	9.3	23.7	2.3	944	*Acartia omorii*	33
	4	8.5	28.2	1.6	1614	*Acartia omorii*	46
	5	8.4	29.9	1.0	2888	*Acartia omorii*	49
	6	9.1	27.4	0.8	2123	*Acartia omorii*	32
	7	8.7	26.9	1.3	1673	*Paraclanus parvus*	41
	8	9.0	26.9	1.1	2159	*Paraclanus parvus*	30
	9	9.0	26.1	1.0	2690	*Paraclanus parvus*	35
Spring May 2015	1	19.8	0.0	5.0	2265	*Pseudodiaptomus koreanus*	88
	2	19.8	4.7	2.0	175	*Pseudodiaptomus koreanus*; *Tortanus dextrilobatus*	46
	3	19.0	11.2	0.9	324	*Acartia omorii*	53
	4	17.4	27.2	6.2	326	*Corycaeus affinis*	38
	5	17.0	30.1	2.2	266	*Corycaeus affinis*	52
	6	17.0	32.2	6.8	358	*Corycaeus affinis*; *Calanus sinicus*	41
	7	18.0	32.7	5.3	148	*Corycaeus affinis*	73
	8	16.5	32.9	3.8	139	*Corycaeus affinis*	41
	9	16.5	32.8	2.7	150	*Acartia omorii*	81
Summer August 2015	1	26.8	0.4	1.0	53	*Tortanus dextrilobatus*	79
	2	27.4	10.6	4.3	3220	*Tortanus dextrilobatus*	58
	3	27.1	20.5	4.5	784	*Acartia ohtuskai*	71
	4	25.8	28.8	1.6	1401	*Acartia ohtuskai*	62
	5	23.7	32.2	2.8	366	*Acartia ohtuskai*	37
	6	23.9	32.2	2.9	129	*Acartia erythraea*	67
	7	24.1	32.3	2.3	79	*Labidocera rotunda*	60
	8	24.5	32.4	1.6	124	*Acartia erythraea*	93
	9	24.2	32.5	2.4	81	*Acartia erythraea*	55
Autumn November 2015	1	8.8	0.0	0.2	17	*Sinocalanus tellenus*	78
	2	9.9	4.7	0.1	22	*Paracalanus parvus*	32
	3	11.3	15.0	0.5	33	*Paracalanus parvus*	32
	4	12.1	20.9	0.4	32	*Corycaeus affinis*	65
	5	15.4	31.3	0.4	18	*Corycaeus affinis*	62
	6	14.6	31.3	0.4	41	*Corycaeus affinis*	55
	7	14.7	31.8	0.9	113	*Corycaeus affinis*	71
	8	14.8	32.3	1.1	118	*Corycaeus affinis*	30
	9	14.2	32.1	0.4	23	*Corycaeus affinis*	56

5

Table 2: Coefficients (F) and significance levels (p) of the effects of variable predictors on $\delta^{15}N$ of nanoplankton (plankton < 20 μm) and microplankton (plankton > 20 μm) using a Generalized Additive Model test. P-value < 0.05 indicates significance. The symbol 'n.s.' represents no significance.

Predictors	Nanoplankton		Microplankton	
	F	p	F	p
Temperature	5.493	0.013	5.008	0.015
Salinity	2.790	n.s.	5.001	0.011
Ammonia	4.116	0.029	4.521	0.031
Nitrite	1.436	n.s.	2.128	n.s.
Nitrate	3.292	n.s.	7.795	0.010
Chlorophyll a	3.786	0.044	4.159	0.043
Deviance explained	66.3%		73.1%	
R^2	0.526		0.638	

5

Table 3: Coefficients (F) and significance levels (p) of the effects of variable predictors on $\delta^{13}C$ and $\delta^{15}N$ copepods using a Generalized Additive Model test. P-value < 0.05 indicates significance. The symbol ′n.s.′ represents no significance.

Predictors	Copepod $\delta^{13}C$		Copepod $\delta^{15}N$	
	F	p	F	p
Temperature	7.887	0.005	1.03	n.s.
Salinity	0.075	n.s.	13.641	<0.001
Chlorophyll a	6.193	0.008	3.272	0.047
Nanoplankton $\delta^{13}C$	16.411	<0.001		
Nanoplankton $\delta^{15}N$			1.086	n.s.
Microplankton $\delta^{13}C$	1.465	n.s.		
Microplankton $\delta^{15}N$			3.456	0.034
Deviance explained	92.7%		76.9%	
AIC test	0.894		0.686	
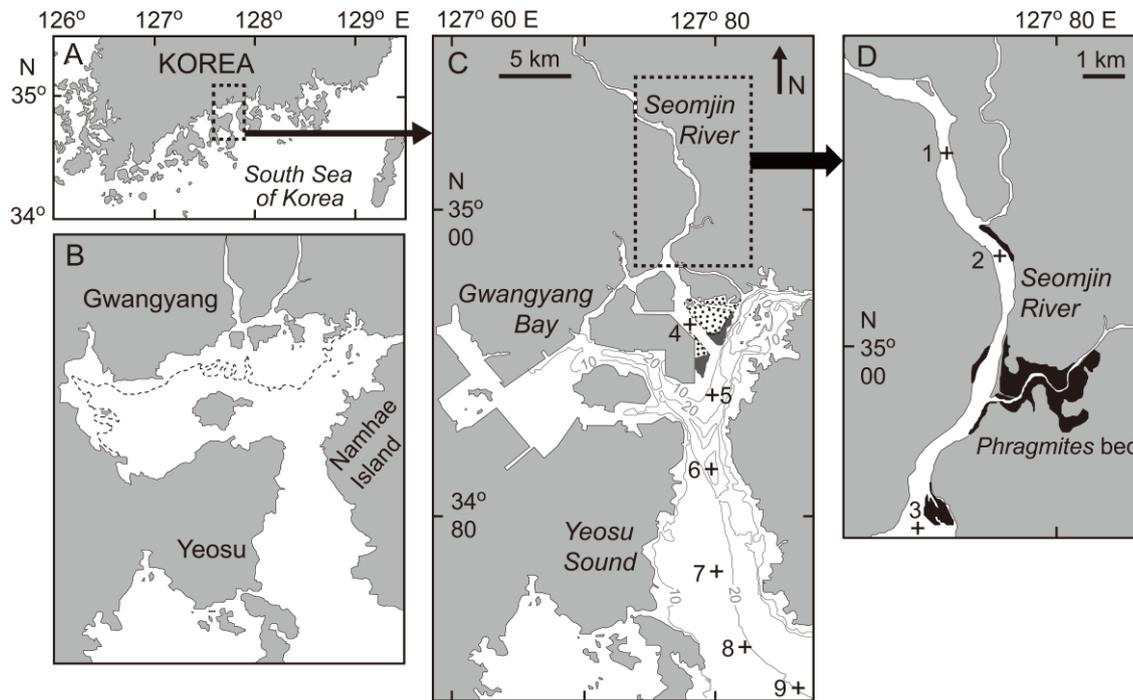
Figure 1: Map showing the location of Gwangyang Bay (A), the appearance of the bay before the reclamation of tidal flats in 1982 (B), the sampling stations in the bay (C), and in the estuarine channel (D). The broken line represents the lowest water line (B); the dotted areas show intertidal beds, the dark gray areas *Zostera* beds (C); and the darker areas *Phragmites* beds (D).

5
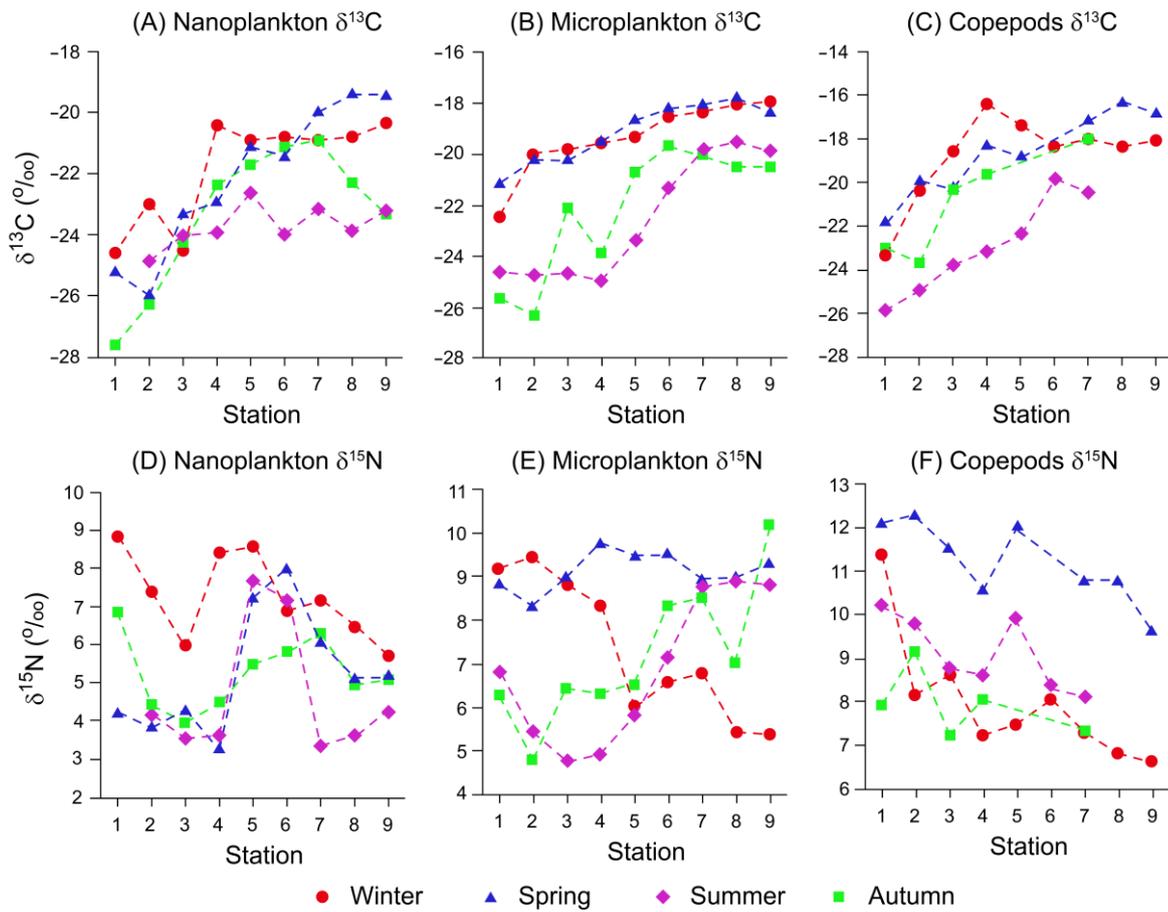
Figure 2: Temporal and spatial variations in plankton $\delta^{13}C$ (‰) and $\delta^{15}N$ (‰).
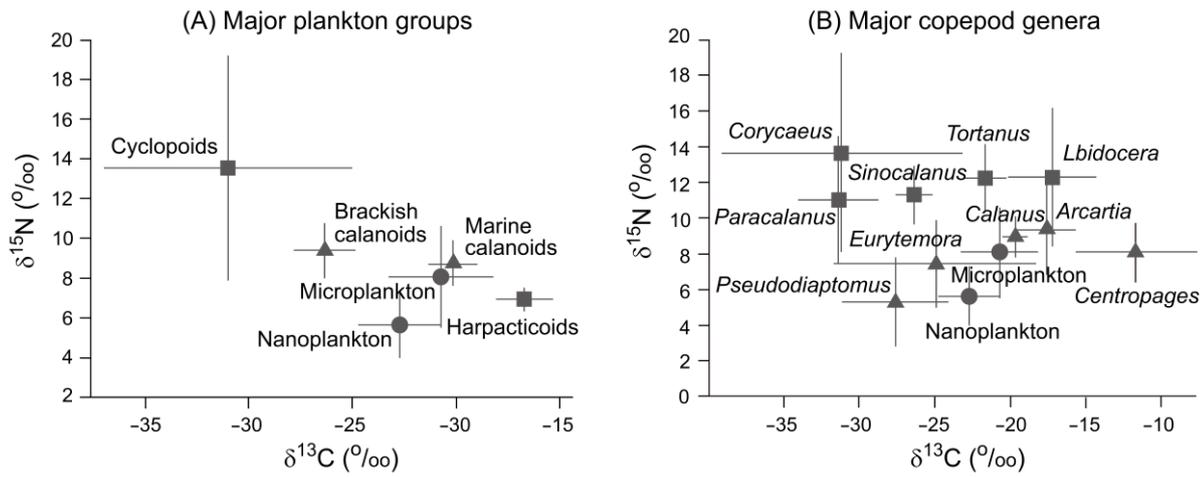
Figure 3: Bi-plots of major plankton group and genus isotopes in Gwangyang Bay.
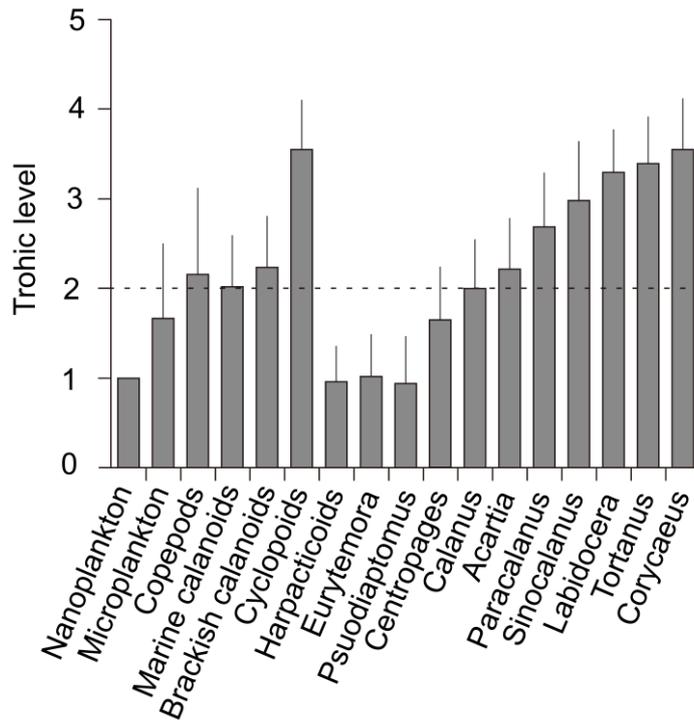
Figure 4: Trophic levels (TLs) of different groups. Nanoplankton were set as TL = 1, while consumers' trophic levels were calculated as: $TL = 1 + (\delta^{15}N_{consumer} - \delta^{15}N_{Nanoplakton})/3$. **The reference line indicates the herbivores relative to nanoplankton. However, nanoplankton here might not be truly primary producers as the bulk samples might include heterotrophic flagellates, dinoflagellates, and ciliates, which we could not separate from the collected samples.**
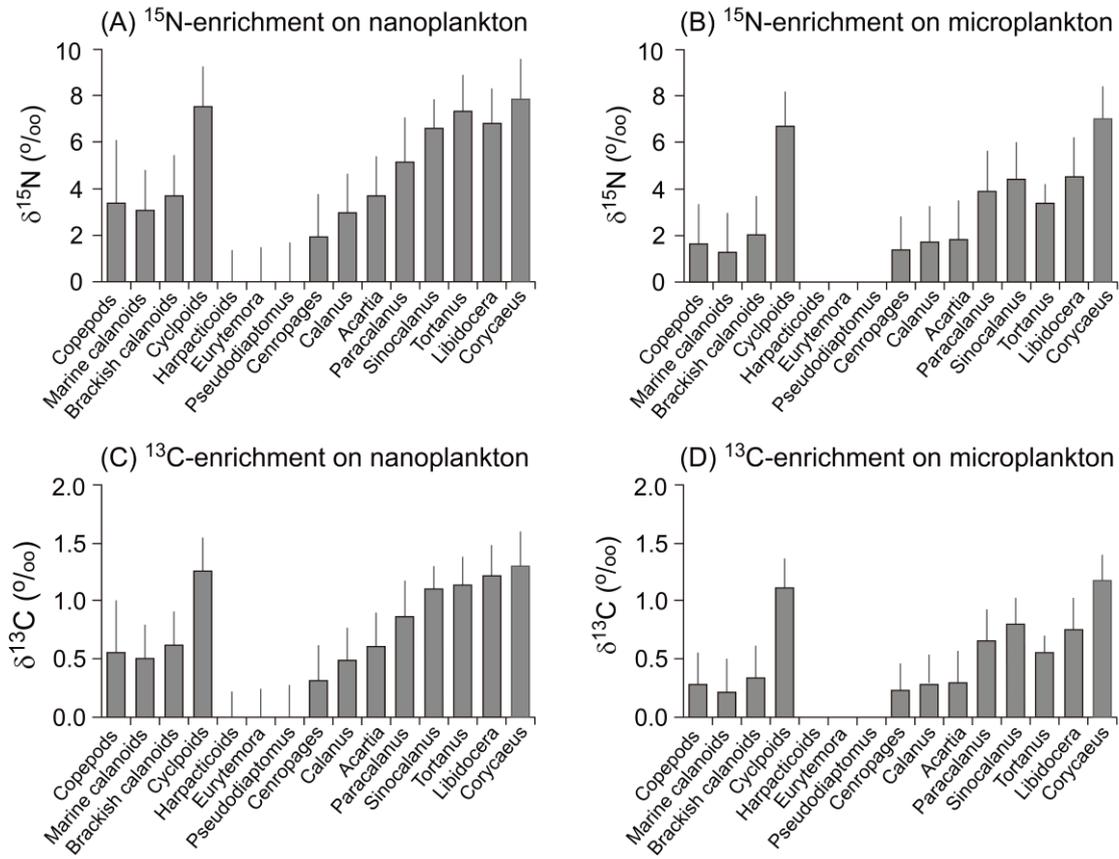
Figure 5: Trophic enrichment (or fractionation factor) from basal food items (nanoplankton: A and C; microplankton: B and D), based on the difference of each sample's δ15N between higher trophic level to lower trophic level; a 0.5‰ per one trophic level was used to calculate the δ13C enrichment for each group. Reference lines indicate mean values from all groups.

5
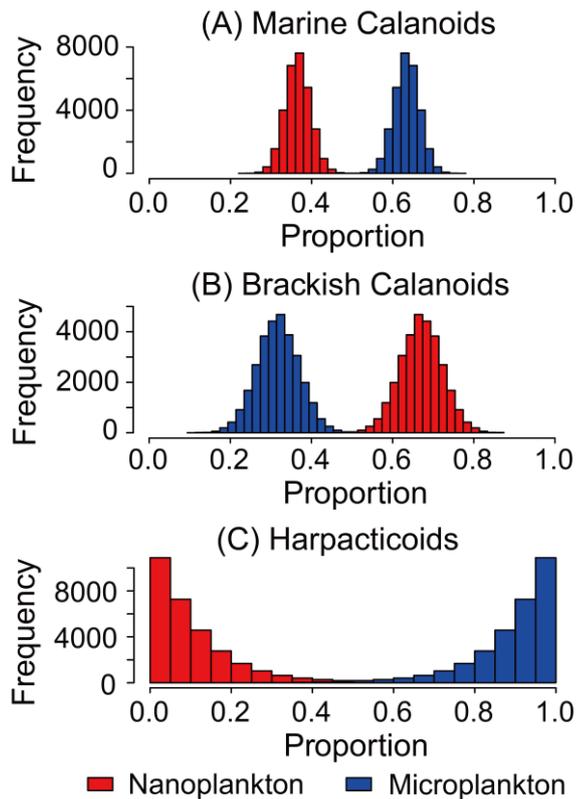
Figure 6: Comparison of the dietary compositions of major copepod groups **(A) Marine calanoids**, including *Acartia hudsonica*, *Acartia o*morii, *Bestiolina coreana*, *Calanus sinicus*, *Clausocalanus furcatus*, *Centropages abdominalis*, *Centropages dorsispinatus*, *Paracalanus aculeatus*, *Paraeuchaeta plana*, *Labidocera rotunda*, *Labidocera euchaeta*, *Tortanus dextrilobatus* and *Tortanus forcipatus*; **(B) Brackish calanoids**, including *Acartia ohtsukai*, *Acartia erythraea*, *Eurytemora Pacifica*, *Paracalanus parvus*, *Pseudodiaptomus koreanus*, *Pseudodiaptomus marinus* and *Sinocalanus tenellus*; and **(C) Harpacticoids.**
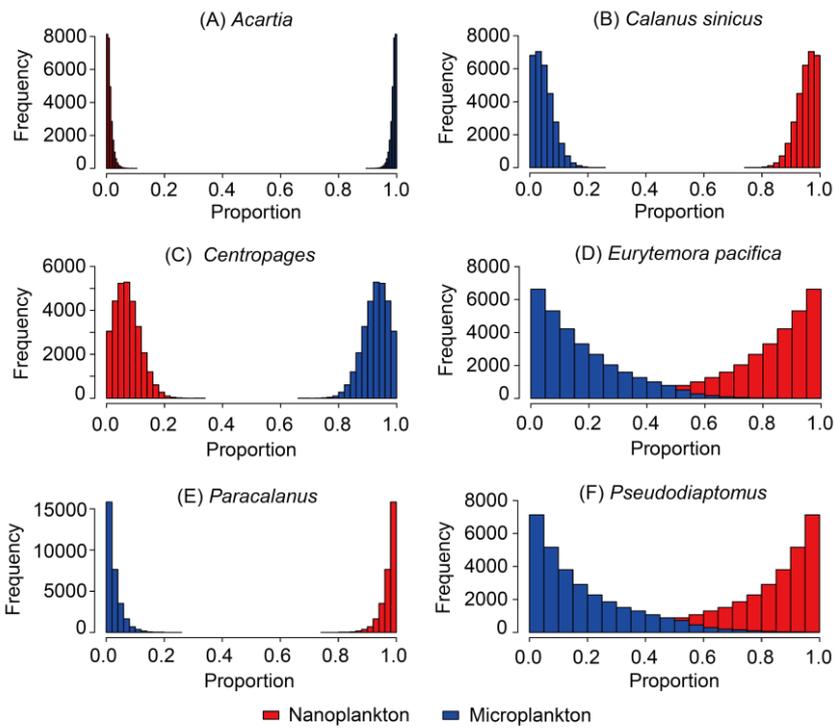
Figure 7: Comparison of the dietary compositions of major omnivorous copepod genera.

5
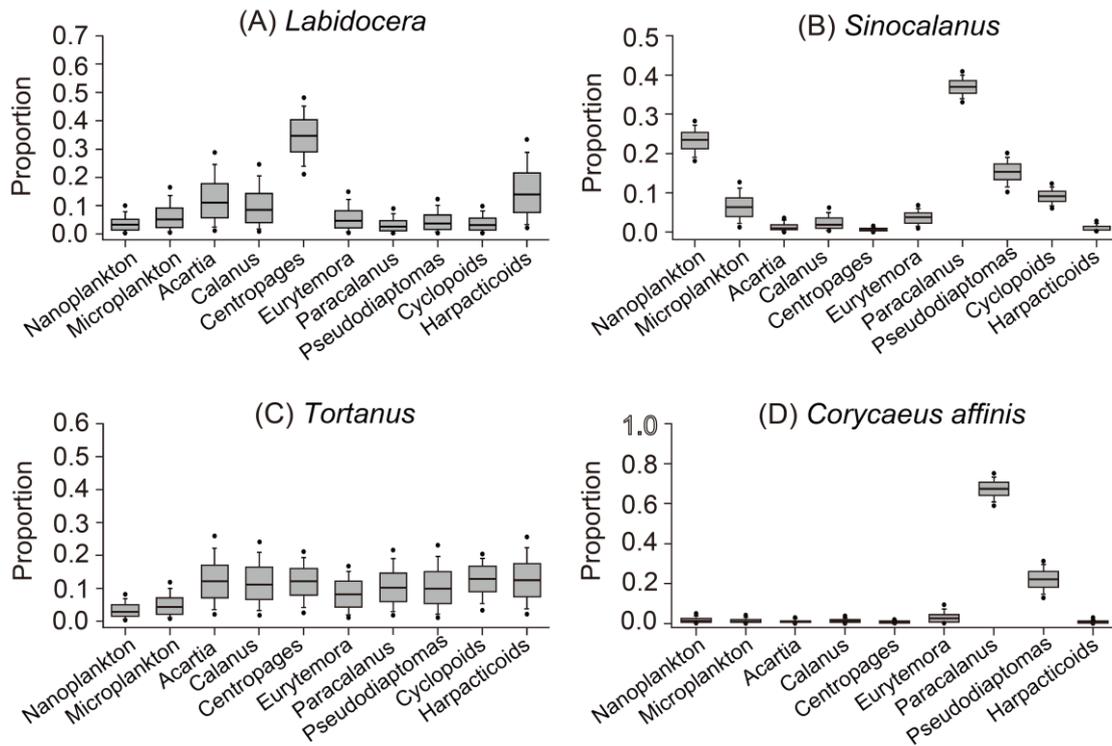
Figure 8: Comparison of the dietary composition of major carnivorous genera. Credibility intervals of 95% (dots), 75% (whiskers), and 25% (boxes) and mean values (lines in the boxes) are shown in boxplots for each source.

5
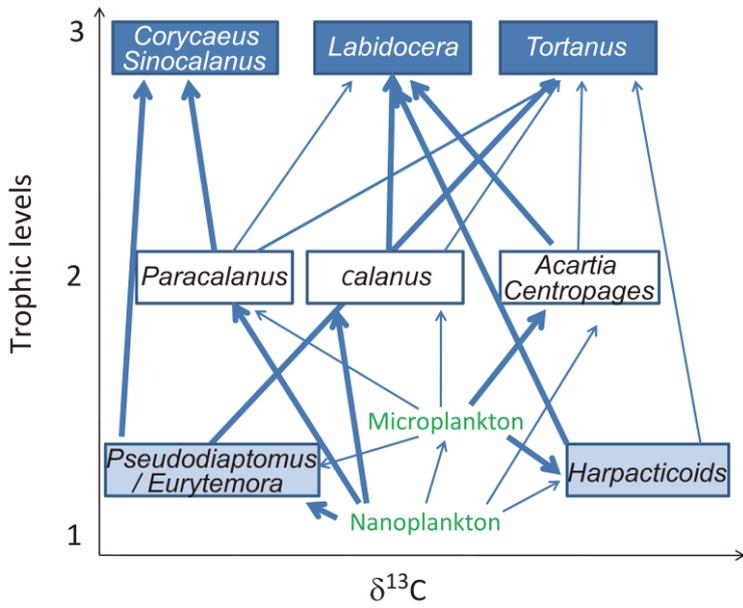
Figure 9: A simplified energy flow figures of Gwangyang Bay plankton and copepods. Arrows indicate feeding relationships. Strong arrows indicate feeding preference.